Computers, Algorithms and Frameworks for Fusion

John Wright - PSFC@MIT

August 26, 2015 - Princeton Plasma Physics Laboratory

Computers and Infrastructure

Cluster infrastructure at PSFC has advanced with technology

Design and Maintenance Team: Ted Baker, Darin Ernst and John Wright

Marshall Theory cluster (2002-2008):

- Cost: ≈ $100k for 48 cores.
- Disk space: 80 GB with 1 GB/core
- Network: Myrinet with ethernet backbone
- Lesson learned: low latency network needed for performance

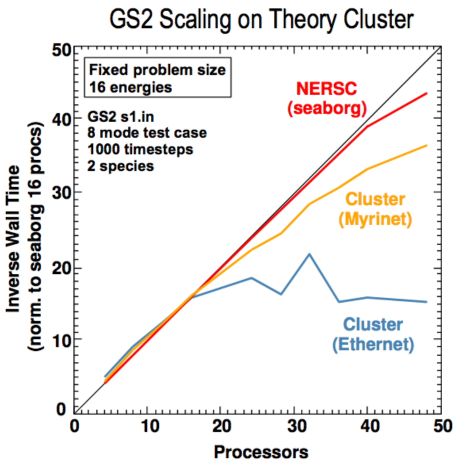

Performance:

- Myrinet needed to access full performance. Has 1/10 latency of Ethernet. 2.4 x faster than Myrinet.
- Performance on 48 cores comparable to Nersc (at the time)

Cluster infrastructure at PSFC has advanced with technology

Design and Maintenance Team: Ted Baker, Darin Ernst and John Wright

Loki PSFC cluster (2007-present):

- Cost: $\approx$ \$300k for 600 cores.
- Disk space: 20 TB with 1.5 GB/core
- Network: Infiniband with gigabit backbone
- Lesson learned: Serial file system (NFS) can be saturated by large number ($>$ 100) of simultaneous I/O processes. Need parallel file system or local disks.

Performance:

- High resolution full wave lower hybrid simulation took 6.5 *days* on Marshall takes 4.5 *hours* on loki. $>$ 10x speedup over previous cluster (2x from IB)

- Team receive MIT 'Infinite Mile Award' for efforts with loki.

Massachusetts Green High Performance Computing Center - MGHPCC

- A consortium of universities and the state of Massachusetts
- 90 000 sq ft, 15 MW, house up to 20 000 nodes, 70% hydro power, 90 mi west of Boston
- Spent a summer working with MIT MGHPCC lead evaluating technologies and coordinating relocation of campus clusters
- Likely location for next generation PSFC cluster with $\approx$ 3000 cores and parallel file system.

Computers - Summary

- Networks and filesystems are critical for even medium scale (100s of cores) parallel simulations.
- Increased computing capability can make different workflows possible - expensive models become reduced, grand challenges become ensembles.
- Small jobs involving a few nodes can get by with NFS and gigabit networks - possible cost savings in architecture.
- Remote facilities may be needed for largest clusters and we need to overcome remote access issues to cycles and data while maintaining security.

Algorithms for Efficient Model Solutions

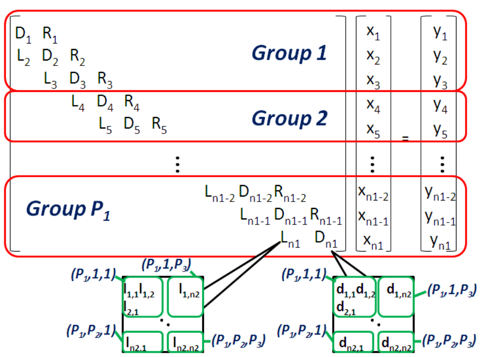

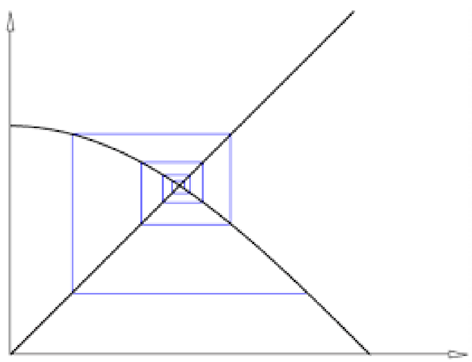

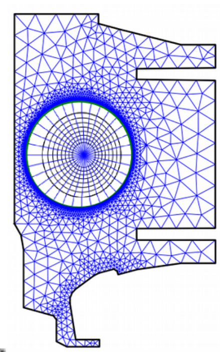

Motivation and Introduction to the Problem

Radio frequency waves in plasmas are an important tool for profile control via heating and current drive to maintain the magnetic equilibrium.

- Ion cyclotron (IC) waves - affect ion distribution: minority tail
- Lower hybrid (LH) waves - affect electron distribution: quasilinear plateau

These waves may modify the particle distribution functions which in turn affects the wave dielectric.

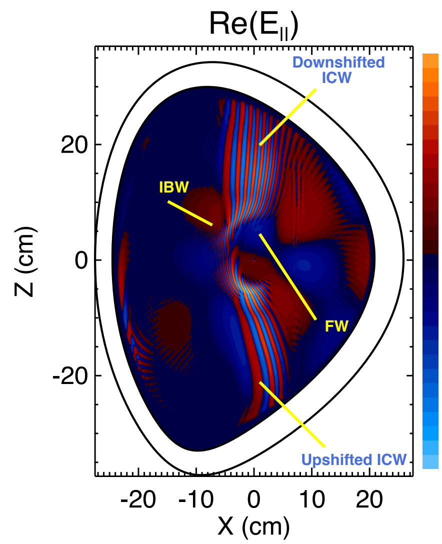

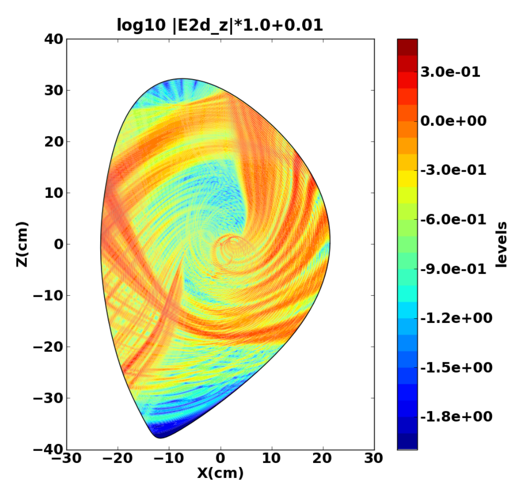

Resolution requirements determined by wave dielectric properties

- The `TORIC` dielectric models are implemented for ion cyclotron and lower hybrid range of frequencies.
- ICRF includes the Ion Bernstein waves (IBW), Ion Cyclotron waves (ICW), Fast waves (FW) and High Harmonic Fast Waves (HHFW).
- LHRF includes the fast and slow Lower Hybrid waves.
- Solution in finite element and Fourier basis: $\mathbf{E}(r,\theta,\phi) = \sum_{m,n} \mathbf{E}_{m,n}(r) \exp\left(im\theta + in\phi\right)$
- Resolution needed depends on the specific wave scenario:
  - ICRF Mode Conversion (MC) - presence of IBW implies $k_\perp \rho_i \simeq 1$ and if $k_\perp \sim \frac{m}{r}$, then $1 \simeq \rho_i k_\perp \sim \rho_i \frac{m}{r} => M_{\mathrm{max}} \approx \mathbf{255}$, for typical device parameters.
  - LHRF dispersion yields: $\frac{\omega_{\mathrm{pe}}}{\omega} k_\| \sim k_\perp \sim \frac{m}{r} \rightsquigarrow M_{\mathrm{max}} \sim \mathbf{1000}$

Aside: TORIC in the US is result of a long collaboration with IPP

- As graduate student at PPPL, worked on ICRF current drive in predecessor, FISIC, resulted in first fullwave ICRF fast wave current drive calculation
- At MIT, I established the first source code repository for TORIC, moving beyond named directory versions for the first time. Repo was used by MIT, PPPL/Transp, and IPP (eventually replaced by svn repo at IPP)
- With Ed D'Azevedo at ORNL, I did the first parallelization of TORIC at the block level and in the power reconstruction - but that only got us so far . . .

Dense matrix solves

Discretization results in Large Matrix with very large Blocks

$$\underset{\rightrightarrows}{\mathbf{A}} \cdot \mathbf{E} = \mathbf{J}_A \text{ where } \underset{\rightrightarrows}{\mathbf{A}} = \begin{pmatrix} \mathbf{D}_1 & \mathbf{U}_1 & \mathbf{0} & \mathbf{0} & \mathbf{0} \\ \mathbf{L}_2 & \mathbf{D}_2 & \mathbf{U}_2 & \mathbf{0} & \mathbf{0} \\ \mathbf{0} & \ddots & \ddots & \ddots & \mathbf{0} \\ \mathbf{0} & \mathbf{0} & \mathbf{L}_{Nm-1} & \mathbf{D}_{Nm-1} & \mathbf{U}_{Nm-1} \\ \mathbf{0} & \mathbf{0} & \mathbf{0} & \mathbf{L}_{Nm} & \mathbf{D}_{Nm} \end{pmatrix}$$

- Discretizing the BVP produces a matrix equation. The blocks, **L**, **D**, and **U** are each dense matrices of size $O(6Nm)^2$.
- The individual $3N_r$ blocks are distributed across the processors and inverted using `(SCA)LaPack` to do an **LU** decomposition.
- Processor memory limitations on simulation sizes are removed by using an out-of-core technique in which block inverses are stored on local disks.(out-of-core dates back to original serial code)

Multiple contexts used to increase parallelism.

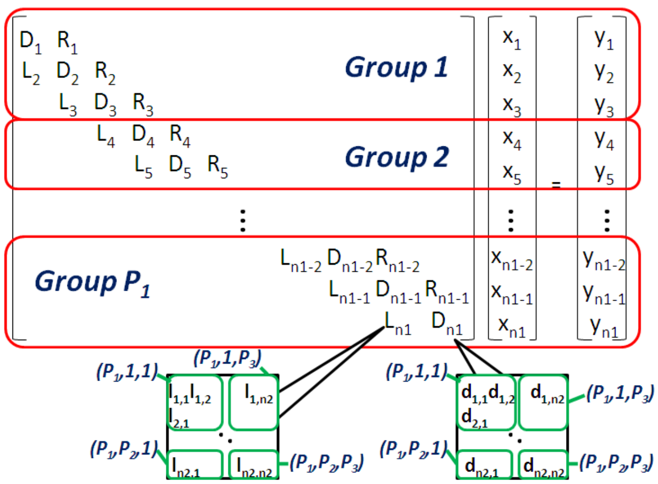

- Individual blocks are distributed with small group of processors
- Block rows are distributed among several parallel contexts to form a two level processor grid for solving the block tri-diagonal system.
- A combination of block-cyclic and divide and conquer is used [Lee and Wright, 2014]
- Floating point work is increased but communication intensity is decreased improving overall weak scalability.

Scaling of new solver

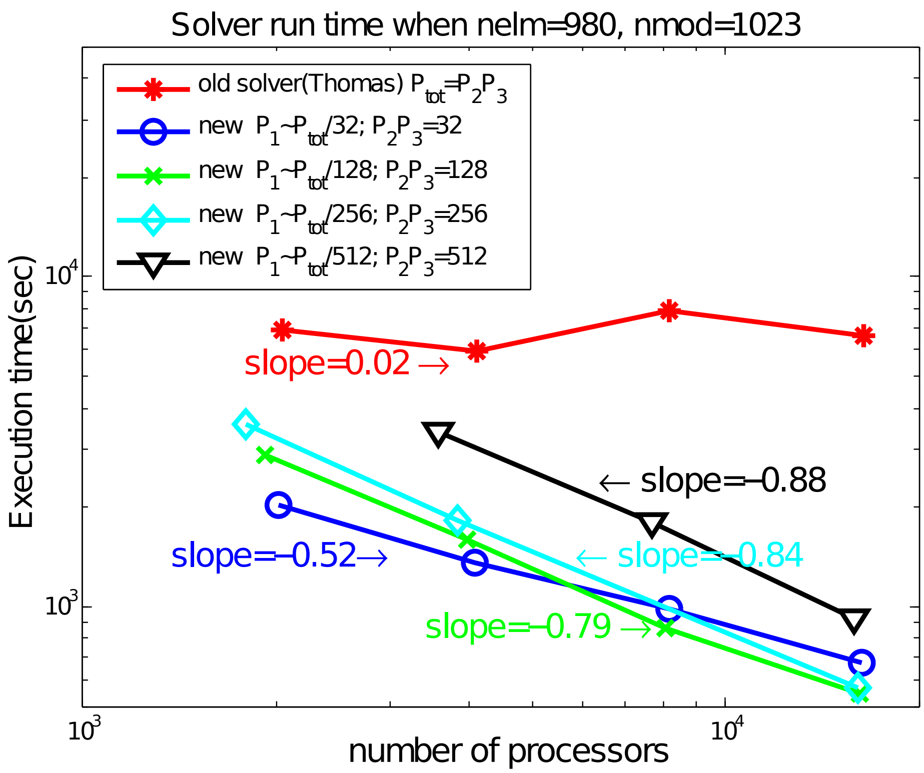

- Red curve showing old parallel solver saturating by 1000 cores
- Other curves show continued scaling of new solver beyond 10 000 cores for different processor group decompositions

Parallel 3D ICRF simulations show three polarizations well separated in space and scale.

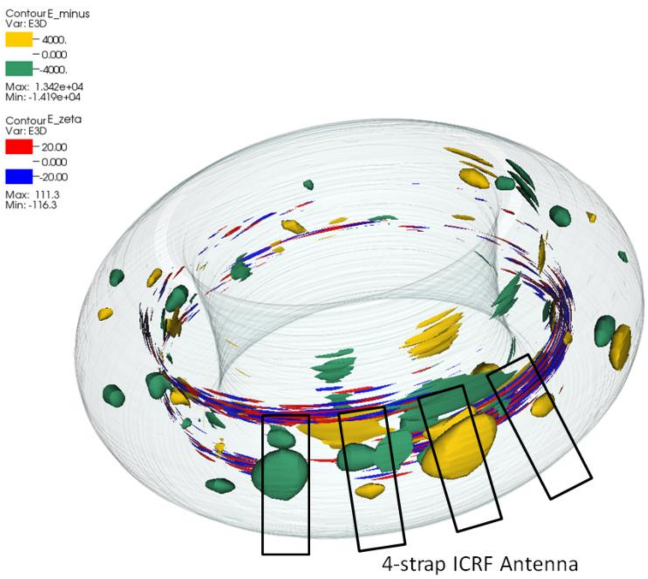

[J-P Lee]

- In 3D we can see the direction of propagation, particularly of the ICW. The IBW distinguished in this view.
- 3D simulations are important for synthetic Phase Contrast Imaging (PCI) diagnostic.

Three dimensional LH simulations show resonant cone structure in fields.

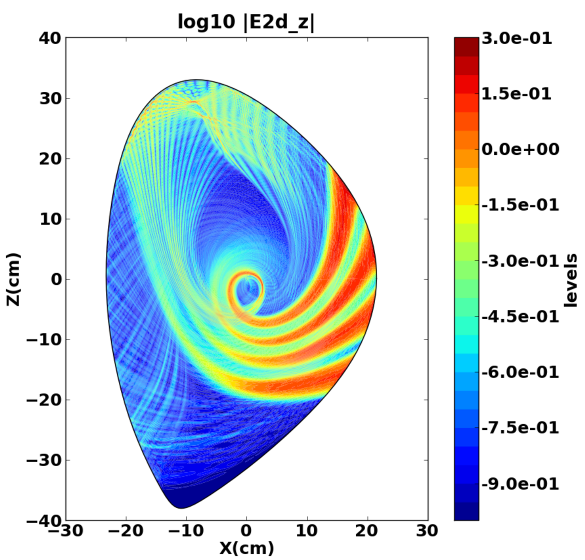

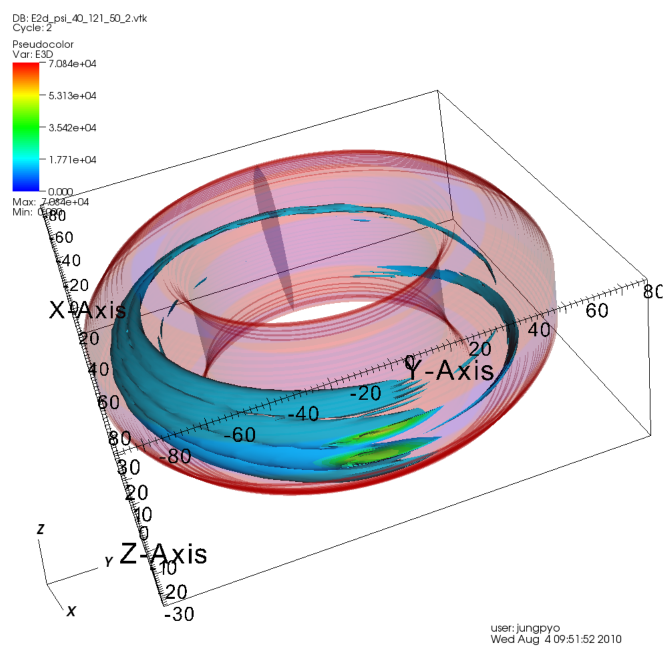

- Converged field patterns shown at 8th iteration between `TORLH` and `CQL3D` in Alcator C-Mod ($n_{\|} = -1.9$).
- 3-D fields obtained by superposing results from 20 toroidal modes.
- 3-D fields exhibit characteristic resonance cone behavior.

Iteration

Equations for rf plasmas are integro-differential, non-linear and time dependent.

- Maxwell's equations in the frequency domain, ω:
  $\nabla\times\nabla\times\mathbf{E} = \frac{\omega^2}{c^2}\left\{\mathbf{E} + \frac{4\pi i}{\omega}\left(\mathbf{J}^P + \mathbf{J}^A\right)\right\}$
- The plasma current response, $\mathbf{J}^P = \int \overleftrightarrow{\sigma}(x, x') \cdot \mathbf{E}(x')$, is an integral operator.
- The dielectric response, $\overleftrightarrow{\sigma}(x, x') \propto \int \hat{H}_u f_0(u) d^3u$ is determined by the distribution function, $f_0(u)$, which in turn is evolved on a much longer timescale (than $1/\omega$) by the Fokker-Planck equation:

$$\partial(\lambda f_0)/\partial t = C(f_0) + D_{\mathrm{ql}}(E^2, f_0).$$

- Solving this nonlinear, coupled set of PDEs requires an iterative process to attain self-consistency.

Iteration for self-consistent coupling

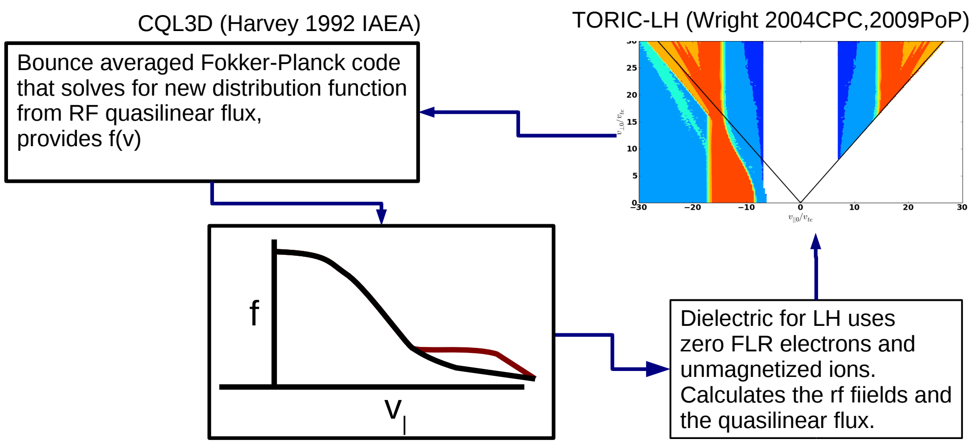

- Simulations use EFIT reconstructed magnetic equilibria.
- Electron distribution functions from iteration with a Fokker-Planck code

- A fixed point iteration scheme is used:

$$f_{n+1} = FP(f_n, Dql_n)$$
$$Dql_{n+1} = WE(f_n)$$

- This technique is known to converge slowly in many instances.
- It can also be unstable in cases of weak ($n_{\|}^2 < 40/T_e$) absorption.

Iteration with Fokker-Planck

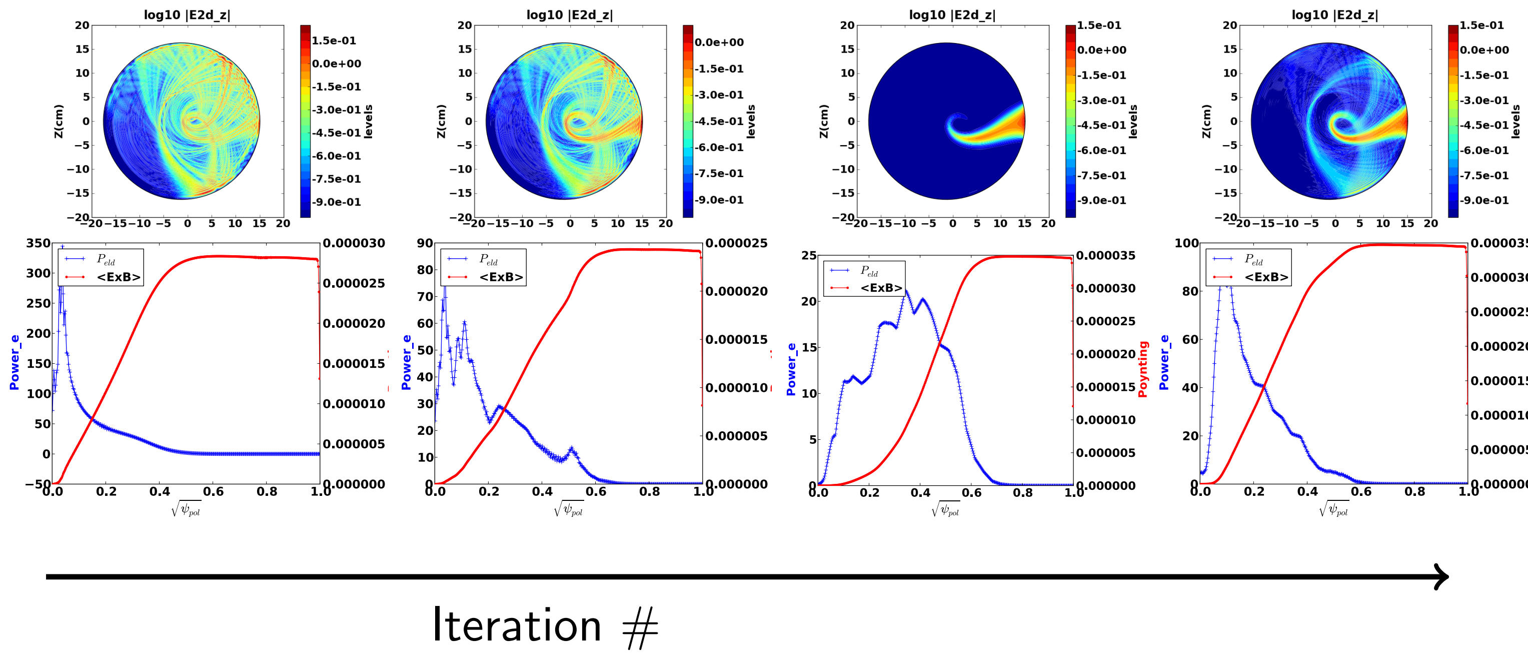

- Converges after some oscillations in damping strength.
- Power of 350 kW generates 150 kA. ($n_{\|} = -2.5$, $T_e = 2.5keV$)
- Resolution, TORLH [Wright *et al.*, 2010] $400N_r \times 255N_m$, CQL3D $60N_r \times 88N_\mu \times 160N_u$

Convergence is difficult, esp in weak damping

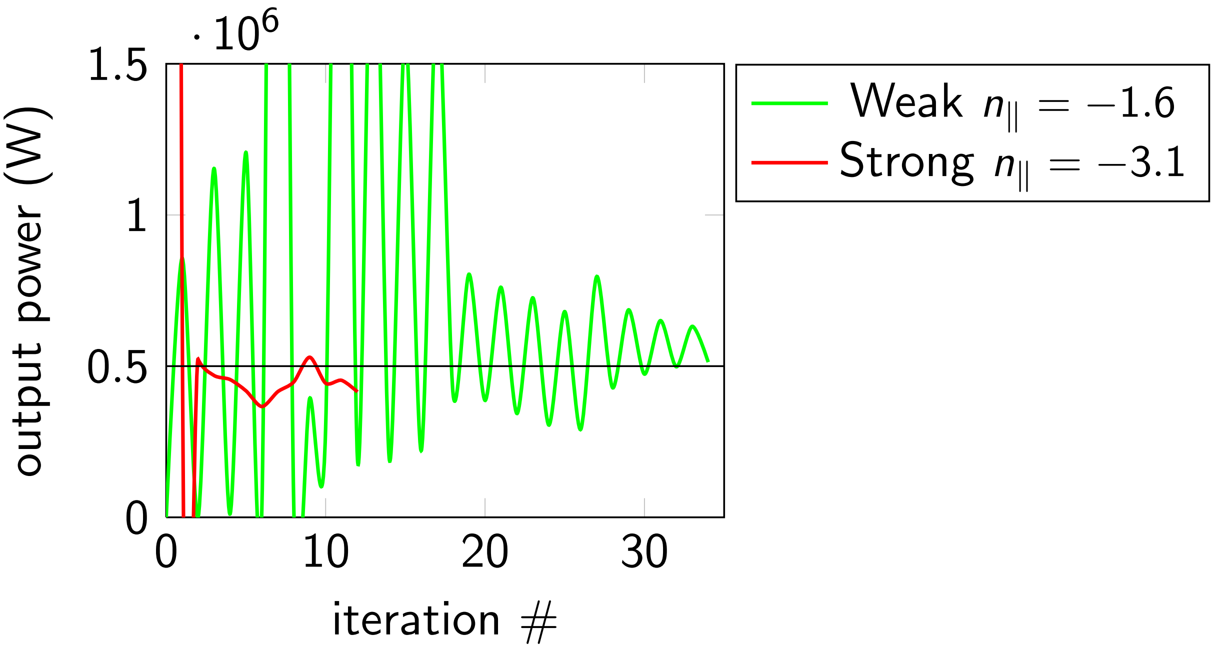

- Target power of 500kW for Alcator C-Mod
- Large oscillations in weak absorption case which eventually settle?

A non-linear iterated system is linear close to solution

- Establish linear behavior by expanding about fixed point.

$$
\begin{aligned}
\Psi(x = s) &= 0 \\
x_{n+1} &= F(x_n) \\
F(x) &= x + \omega A(x)\Psi(x) \\
x_{n+1} &\approx F(s) + F'(s)(x_n - 1) \\
x_{n+1} &= T x_n + b
\end{aligned}
$$

- This is a linear system of size N. Need the inverse.
- $F'(x)$ is the Jacobian, but prefer not to calculate this (ie a Jacobian-free method).
- Key: Solution is a linear superposition of iterations, $s = \sum_{i=1}^{k} c_i x_i$.

Vector Acceleration using Minimum Polynomial Extrapolation (MPE)

- Improves rate of convergence of fixed point iteration methods. Similar to Newton-Krylov and GMRES [Sidi, 2008]
- Our model linear system:

$$x = Tx + b$$

- Sample the actual non-linear system with $k << N$ fixed point (Picard) iterations.
- Form $\sum_{j=0}^{k} c_j u_j = 0$ where $u_j = x_{j+1} - x_j$
- It can be shown that the characteristic polynomial of the system, F, is $P(\lambda) = \sum_{j=0}^{k} c_j \lambda^j$; $c_k = 1$
- Construct inverse through least squares constraints. The solution is given by $s = \sum_{j=0}^{k} c_j x_j$
- The MPE method optimally constructs the solution in the subspace of iterate samples, ie: magic.

Acceleration of LH iteration reduces error in steady state

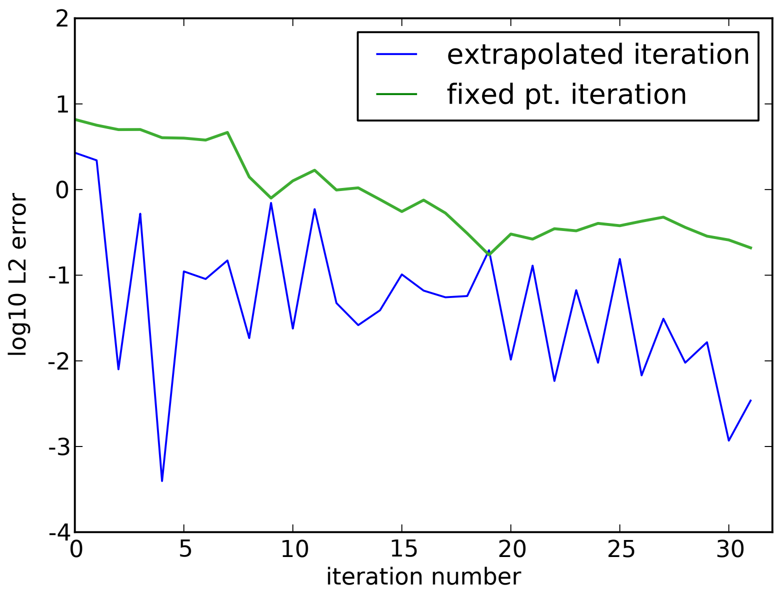

- Vector extrapolation here is applied to continues sets of 7 iterations to show local improvement.
- Refinement of solution takes less than 10 minutes with gain in accuracy of $\gg$ 10 times.
- Power is now accurate to within 1%.

C-Mod $n_\parallel = -1.55$

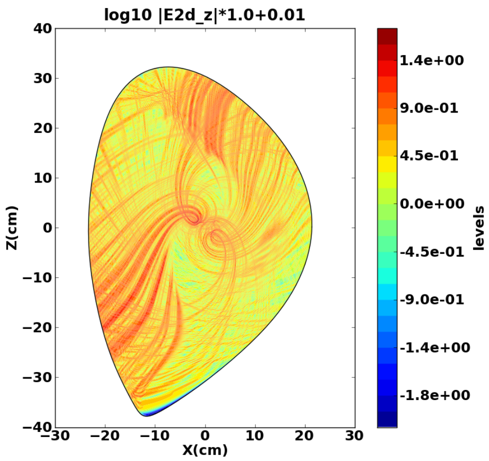

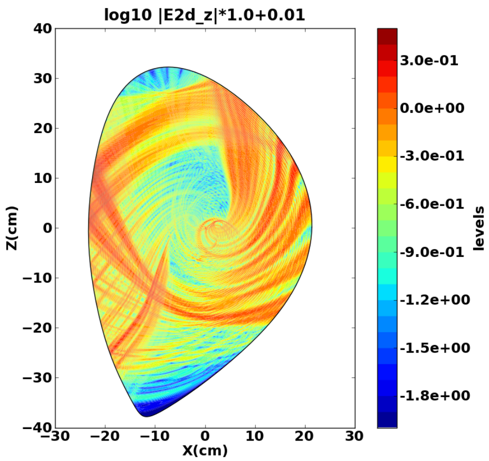

- Upper left initial
- Lower left converged
- Upper right converged spectrum
- Lower right converged power

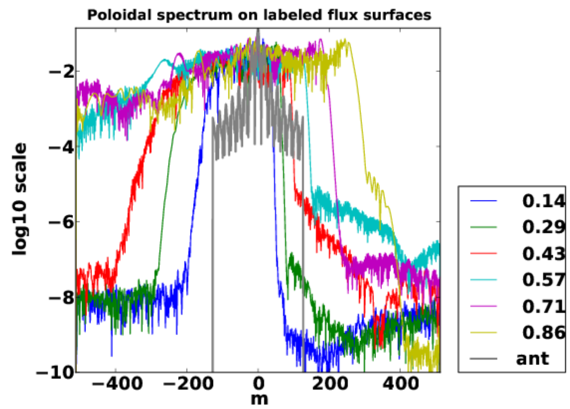

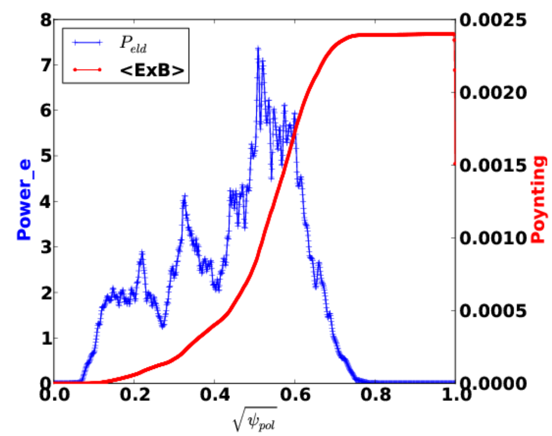

Mode Matching

Goal: introducing realistic SOL boundary plasmas to TORIC ICRF solver

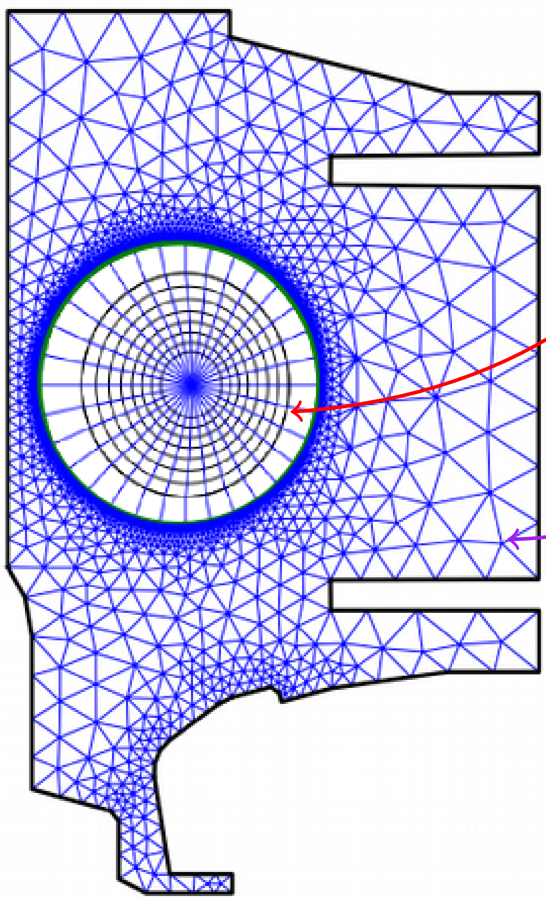

- TORIC
  - Well validated solver for hot core plasma
  - Spectral solver, flux aligned mesh
- SOL plasma
  - Complicated geometry
  - Open field lines
- Can we solve two regions separately and connect them later?
- Solution can be obtained by linear combination of solutions obtained by different boundary values.

[Wright and Shiraiwa, 2015]

Mode Matching technique

- Mode matching method is a particular way of cascading of two linear systems.
- Calculate the separate solutions in regions A and B for different modal excitations. Then superimpose the solutions, so that boundary conditions are satisfied.
- Electric fields match for each mode at interface by construction
- Matching magnetic fields in presence of antenna currents given the matching ampltitudes.

- $(\overleftrightarrow{B}^{\mathtt{IN}} - \overleftrightarrow{B}^{\mathtt{OUT}}) \cdot \mathbf{x} = \mathbf{B}^{\mathtt{ANT}}$
- Where $\overleftrightarrow{B}$ is the array of rf magnetic field responses for each electric field boundary condition and $\mathbf{B}$ is the projection of the antenna created rf magnetic field on the same basis.
- Overhead is $\approx$ a factor of 2:

$$\overleftrightarrow{A}\mathbf{x} = \mathbf{b} \quad \text{order } N^3$$
$$\overleftrightarrow{A}\overleftrightarrow{X} = \overleftrightarrow{B} \quad \text{order } 2N^3$$

[Meneghini and Shiraiwa, US-Japan Workshop on RF Physics (2010), Wright and Shiraiwa RF Topical Conference 2015]

SOL modes excited at domain interface - First 3 modes from excitation in E_ϕ

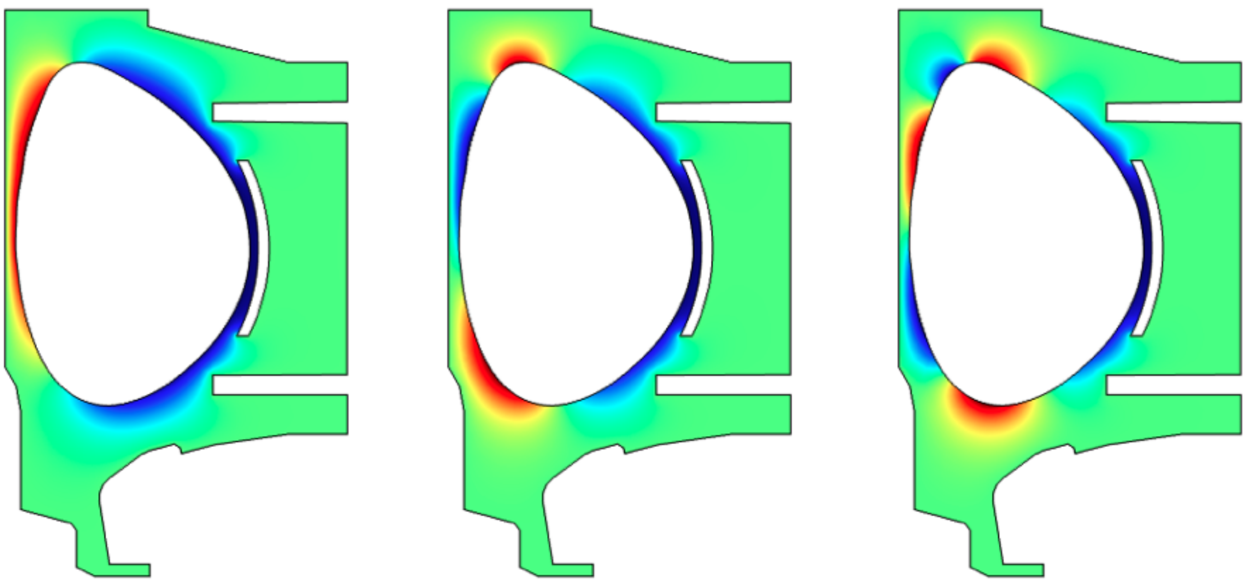

- Poloidal modes excited directly on internal boundary
- No current excited on antenna strap

CORE MODE RESPONSES FOR MATCHING FROM TORIC

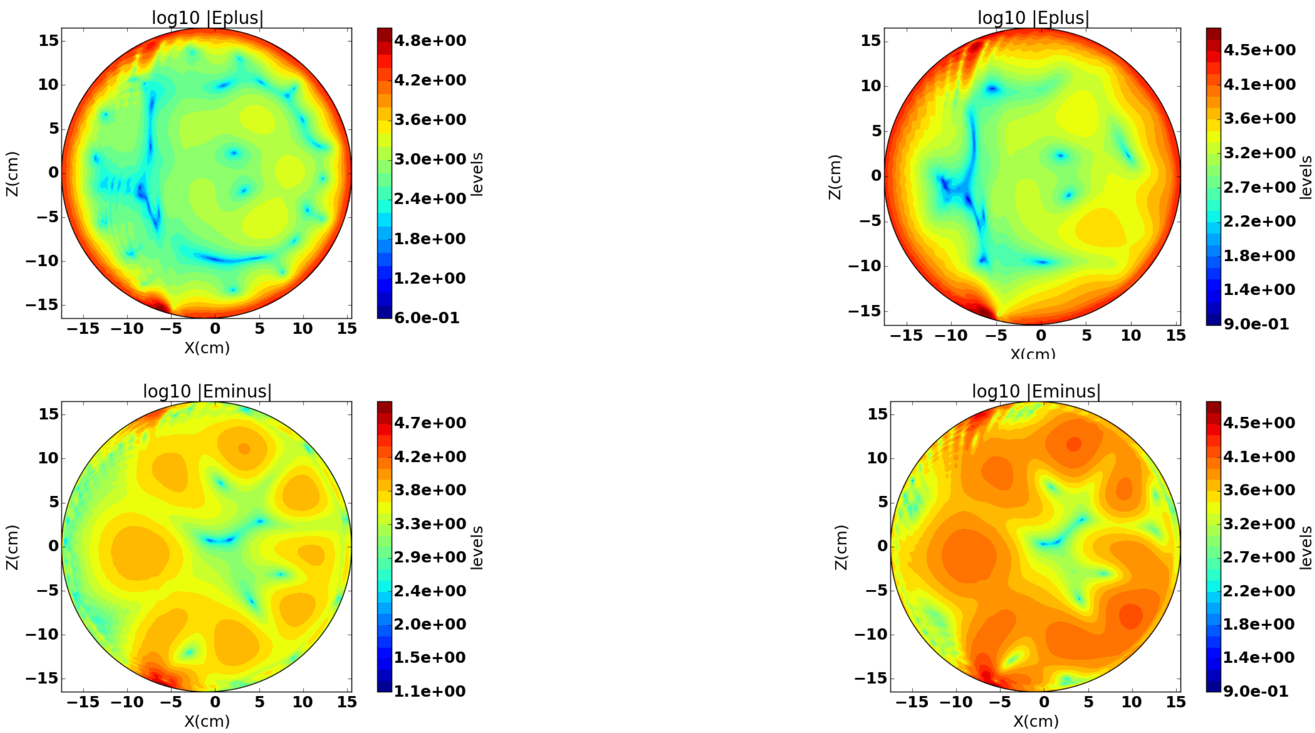

- Responses shown are to pure poloidal mode excitation of poloidal component of electric field (m=16 left, m=8 right)
- Mode matching with fields at matching layer (last closed flux surface) from FEM code with determine reconstruction which should match TORIC reference case.

Reconstructed solution over entire domain

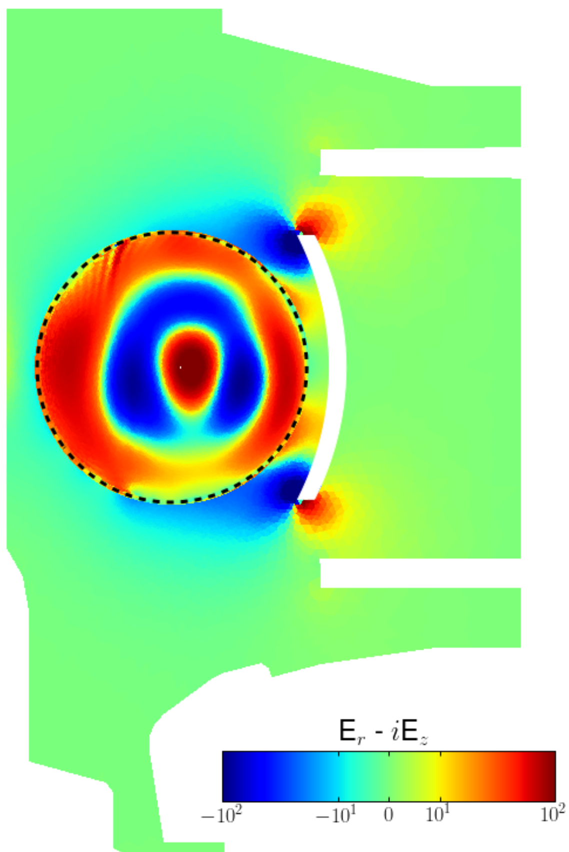

- The combined codes retain hot plasma dielectric in the core while adding important edge geometric effects. This makes available unprecedented fidelity to limiter geometry.
- Applications include modeling of non-conforming antenna placement, accurate limiter geometries and wave propagation in the scrape off layer.
- Extensions to sheath boundary conditions to model far field sheath effects such as may be relevant in NSTX and NSTX-U in HHFW regimes.

... and is very close to reference TORIC case

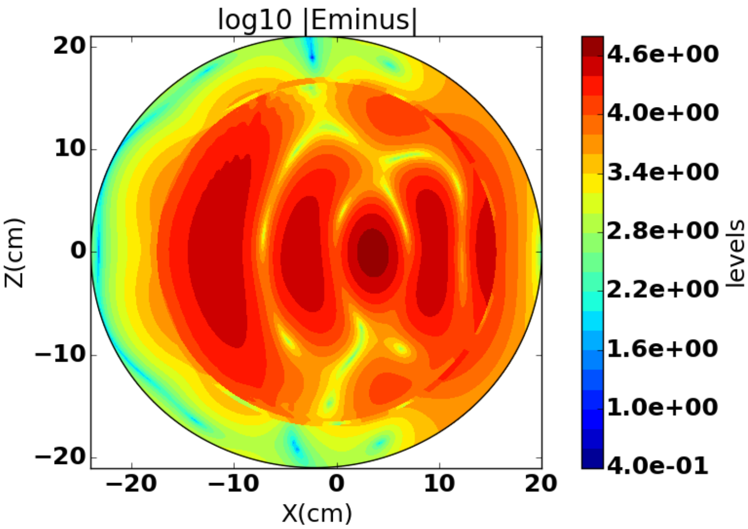

- Minority D(H) ICRF heating case in Alcator C circular geometry
- TORIC scrape off layer fields retained in this plot to show the limited capabilities for edge plasma and for comparison to FEM reconstruction.

Integrated Modeling Fusion Frameworks

Transp

ITER

IMAS

IPS in SWIM project uses a common component architecture

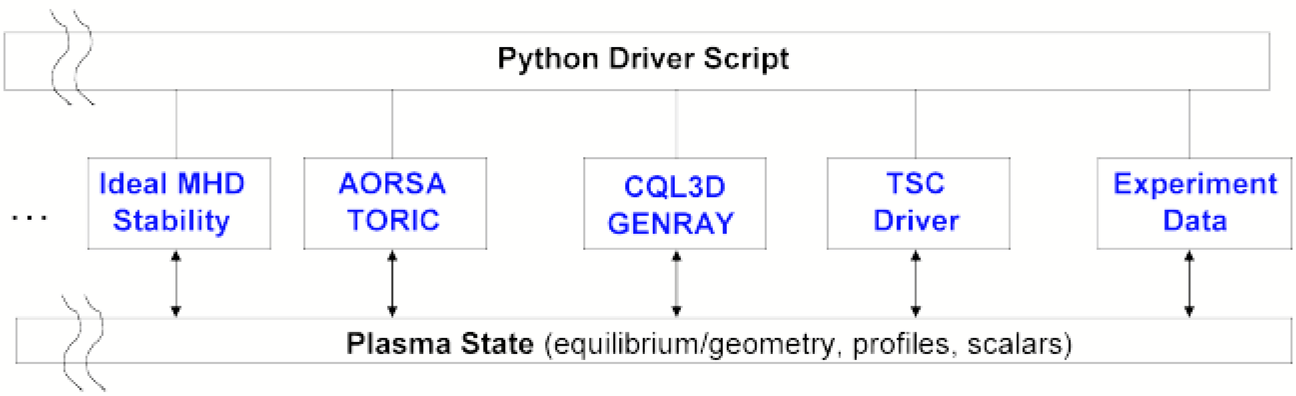

- Define init, step, and finalize methods in python component class wrapper
- IPS uses these methods along with the Plasma State to control workflow
- This loosely coupled design allows rapid incorporation of new physics modules and abstracts the code internals from the framework
- I added the second component, TORIC, to the SWIM project.

Transp

- Plasma State developed by Doug McCune for the SWIM project was used in Transp as a data model.
- Plasma State files are interoperable between the IPS and Transp.
- More recently, components including the class wrappers were used to incorporate GENRAY and CQL3D into Transp.
- $\Rightarrow$ Transp has already influenced development of other frameworks and benefiting from them.

ITER, AToM and OMFIT

- Integrated Modelling & Analysis Suite (IMAS)
  - Based on the European ITM framework
  - Provides tight and loose coupling options for components
  - I ported TORIC to ITER compute cluster
  - Next step is to integrate into IMAS framework.
- The SWIM IPS team is part of AToM
- OMFIT is a modeling framework that is part of AToM
- Workflows in both SWIM and OMFIT have been recorded using a new tool, MPO:

Metadata, Provenance and Ontology Project

- MPO is a collaboration between MIT, GA and LBNL to document any workflow.
- Answer two key questions:
  - Where did a particular piece of data come from?
  - Where was this data used?

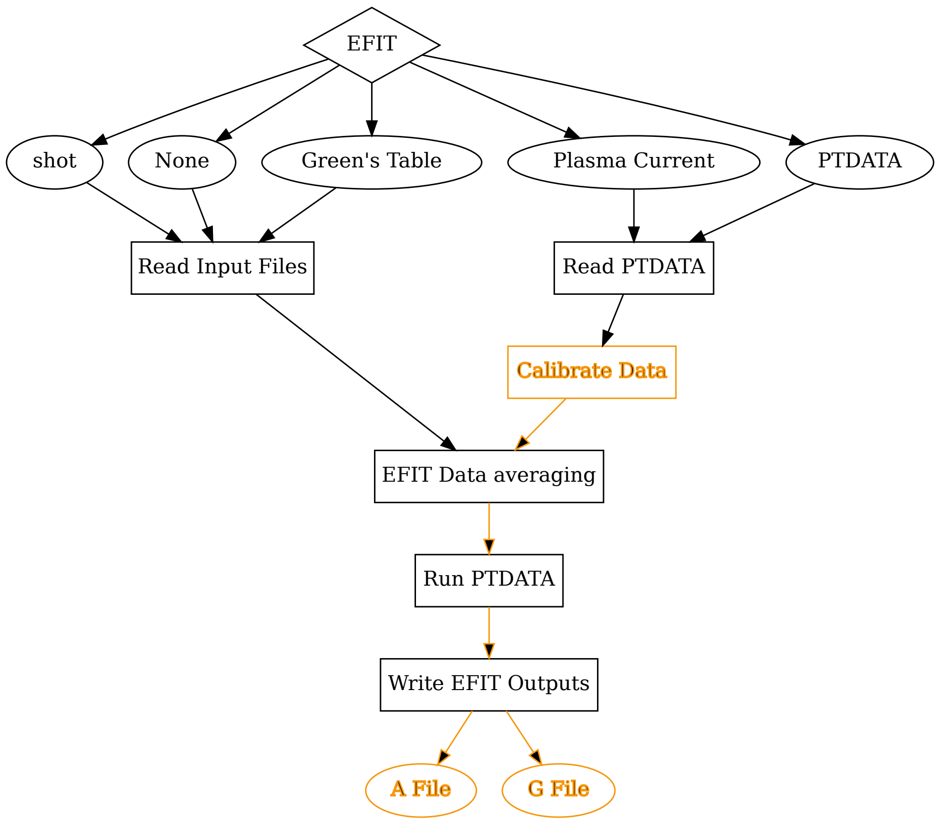

[Wright *et al.*, 2014]

Demo of Search within the MPO

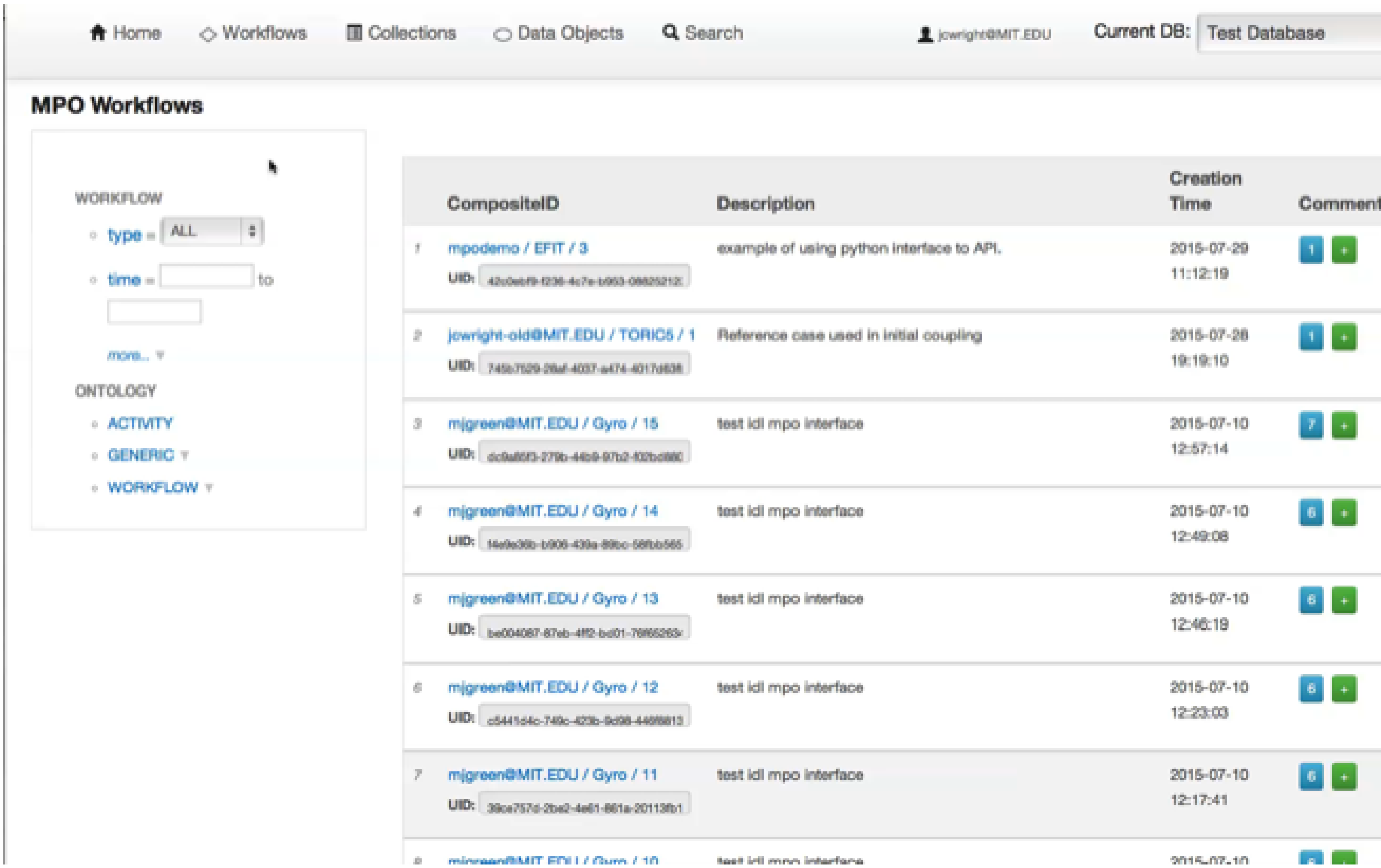

The MPO System is Based on a Multi-Tier Software Architecture

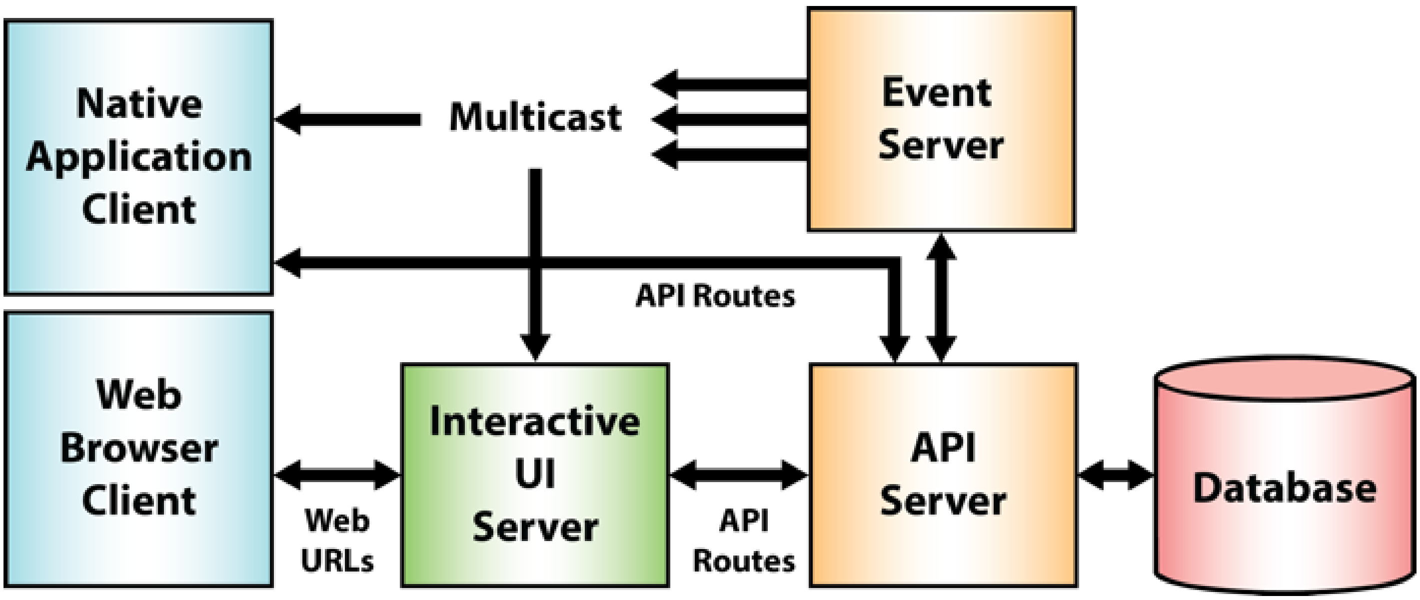

- My key contributations are the native clients and the api server.
- Mediates all communication with database
- Provides a uniform language-independent interface for clients

API uses a ReSTful interface

- "Representational State Transfer" just means all transactions are atomic and independent of the last transaction
- Clients only need HTTPS POST and GET operations to access the MPO.
- Ease of implementation and language agnostic but puts complexity in API server.
- Oriented around construction of URI resources
- Examples:
  - `GET /workflow?user=jwright`
  - `POST /comment {'content':'This is a comment','parent_uid':'3d55-4 ...'}`
  - `GET /workflow/:uid/graph`

Command Line Client For Use in Scripts uses 'meta' command interface

- Familiar to users of other command line interfaces such as svn/git
- Shell scripts and batch scripts can be instrumented
- User can make queries and comments via command line
- Example script or command line session:

```
wid = ‘mpo init --name=EFIT --desc=test‘

oid2 =‘mpo add $wid --parent=$wid --name="Snap file"
     --desc="EFIT input file" --uri=’’\\efit01 : namelist"‘

aid = ‘mpo step $wid --input=$oid2 --name="EFIT exec"
     --desc="Fit equilibrium" ‘

cid = ‘mpo comment $aid "This is the best fit." ‘
```

MPO Summary

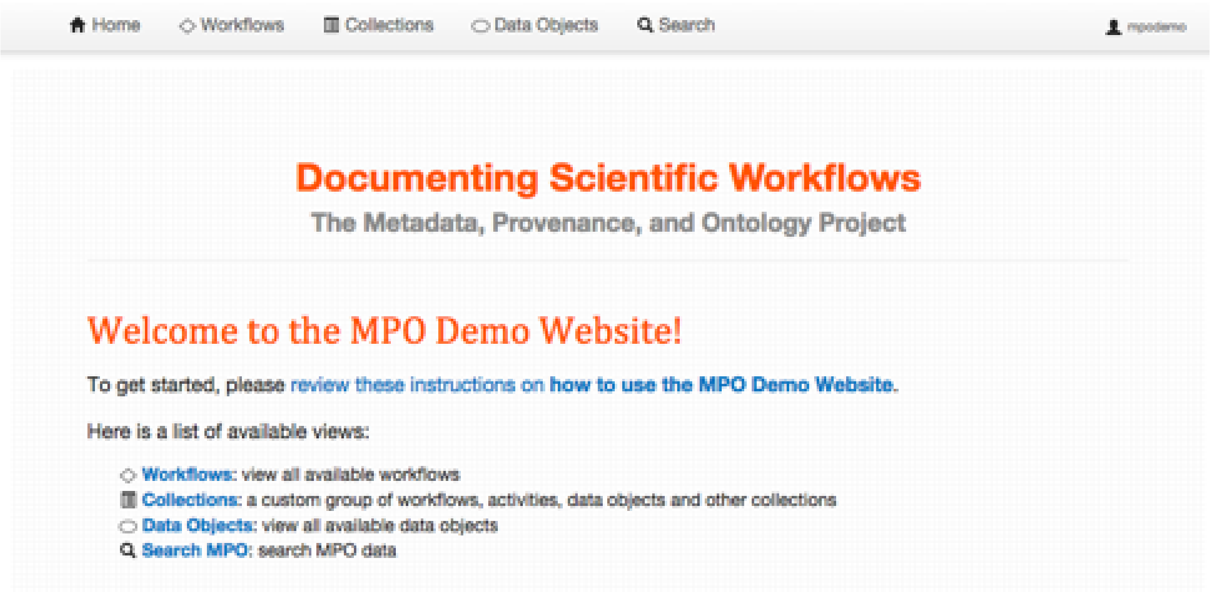

- Use of RESTful API permitted rapid development of web interface and clients in multiple languages.
- Beta release, seeking beta users: mailto:mpo-info@fusion.gat.com
- https://mpo.psfc.mit.edu

Summary

- Computers - Hardware will often dictate what models you can run. More compute intensive components will require more parallel computer resources for Transp and other workflow engines than in the past.
- Algorithms - a good algorithm usually beats a faster computer
- Frameworks - Loose couplings, APIs, and abstractions make tying components together easier.

The End

Backup slides

References and further reading

Bonoli, P. (1984).
Linear Theory of Lower Hybrid Heating.
IEEE Trans. Plasma Sci. **PS-12**, 95–107.

Jaeger, E. F., Berry, L. A., Myra, J. R., Batchelor, D. B., D´Azevedo, E., Bonoli, P. T., Phillips, C. K., Smithe, D. N., DÍppolito, D. A., Carter, M. D., Dumont, R. J., Wright, J. C., and Harvey, R. W. (2003).
Sheared Poloidal Flow Driven by Mode Conversion in Tokamak Plasmas.
Phys. Rev. Lett. **90**, 195001.

Lee, J.-P. and Wright, J. C. (2014).
A block-tridiagonal solver with two-level parallelization for finite element-spectral codes.
Computer Phys. Comm. **185**, 2598.

Lin, Y., Wukitch, S., Bonoli, P., Nelson-Melby, E., Porkolab, M., Wright, J. C., Basse, N., Hubbard, A. E., Irby, J., Lin, L., Marmar, E. S., Mazurenko, A., Mossessian, D., Parisot, A., Rice, J., Wolfe, S., Phillips, C. K., Schilling, G., Wilson, J. R., Phillips, P., and Lynn, A. (2004).
Investigation of ion cyclotron range of frequencies mode conversion at the ion–ion hybrid layer in Alcator C-Mod.
Physics of Plasmas **11**, 2466–2472.

Nelson-Melby, E., Porkolab, M., Bonoli, P. T., Lin, Y., Mazurenko, A., and Wukitch, S. J. (2003).
Experimental Observations of Mode-Converted Ion Cyclotron Waves in a Tokamak Plasma by Phase Contrast Imaging.
Phys. Rev. Lett. **90**, 155004.

Perkins, F. W. (1977).
Heating Tokamaks via the Ion-Cyclotron and Ion-Ion Hybrid Resonances.
Nucl. Fusion **17**, 1197.

Sidi, A. (2008).
Vector extrapolation methods with applications to solution of large systems of equations and to PageRank computations.
Comput. Math. Appl. **56**, 1–24.

Wright, J., Schissel, D. P., Abla, G., Flanagan, S., Greenwald, M., Lee, X., Romosan, A., Shoshani, A.,

Geometry of full wave code, TORIC, is aligned to the magnetic flux geometry for efficiency

- Typical tokamak magnetic equilibrium [Alcator C-Mod]. Showing contours of constant toroidal magnetic flux, (ψ), and poloidal angle, (θ).
- `TORIC` decomposition is spectral in θ and toroidal angle (ϕ) and finite elements in the flux dimension with toroidal axisymmetry assumed.

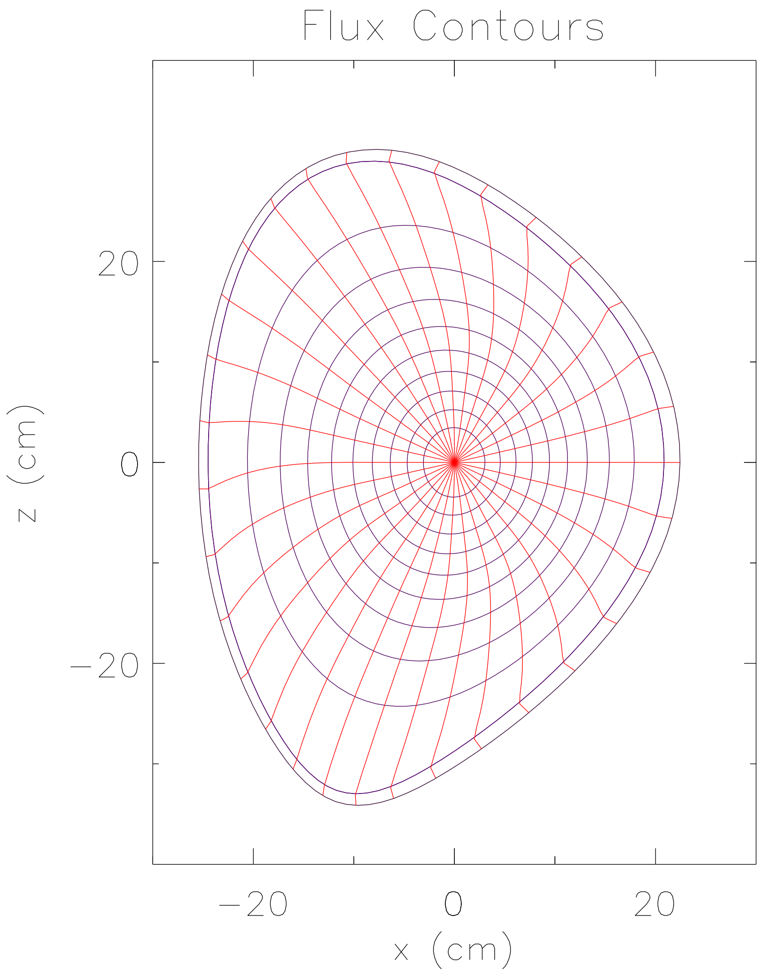

TORIC: FULL WAVE SIMULATIONS

- In the frequency domain Maxwell's equations take the form of a Helmholtz equation with the plasma conductivity, $\overleftrightarrow{\sigma}$, given by a local model,

$$\nabla\times\nabla\times\mathbf{E} = \frac{\omega^2}{c^2}\left\{\mathbf{E} + \frac{4\pi i}{\omega}\left(\mathbf{J}^P + \mathbf{J}^A\right)\right\},$$

$$\text{where } \mathbf{J}^P = \overleftrightarrow{\sigma}\,[f_0(\mathbf{x},\mathbf{v}_\perp,v_\parallel)]\cdot\mathbf{E},$$

  with suitable approximations for $\overleftrightarrow{\sigma}$ in various frequency regimes.
- TORIC solves for the wave electric field in discrete basis using Fourier in flux surface and Hermite finite elements in radial dimension:

$$\mathbf{E}(\mathbf{x}) = \sum_m \mathbf{E}_m(\psi)\exp\left(im\theta + in\phi\right)$$

- This results in a block tridiagonal stiffness matrix, where each block is $(6N_m)^2$, with $3N_r$ blocks. It is solved with a parallel divide and conquer tridiagonal algorithm combined with a parallel LU decomposition of the blocks. TORIC has been run on up to 16000 processors with good strong scaling performance.

Simplified view of ICRF physics

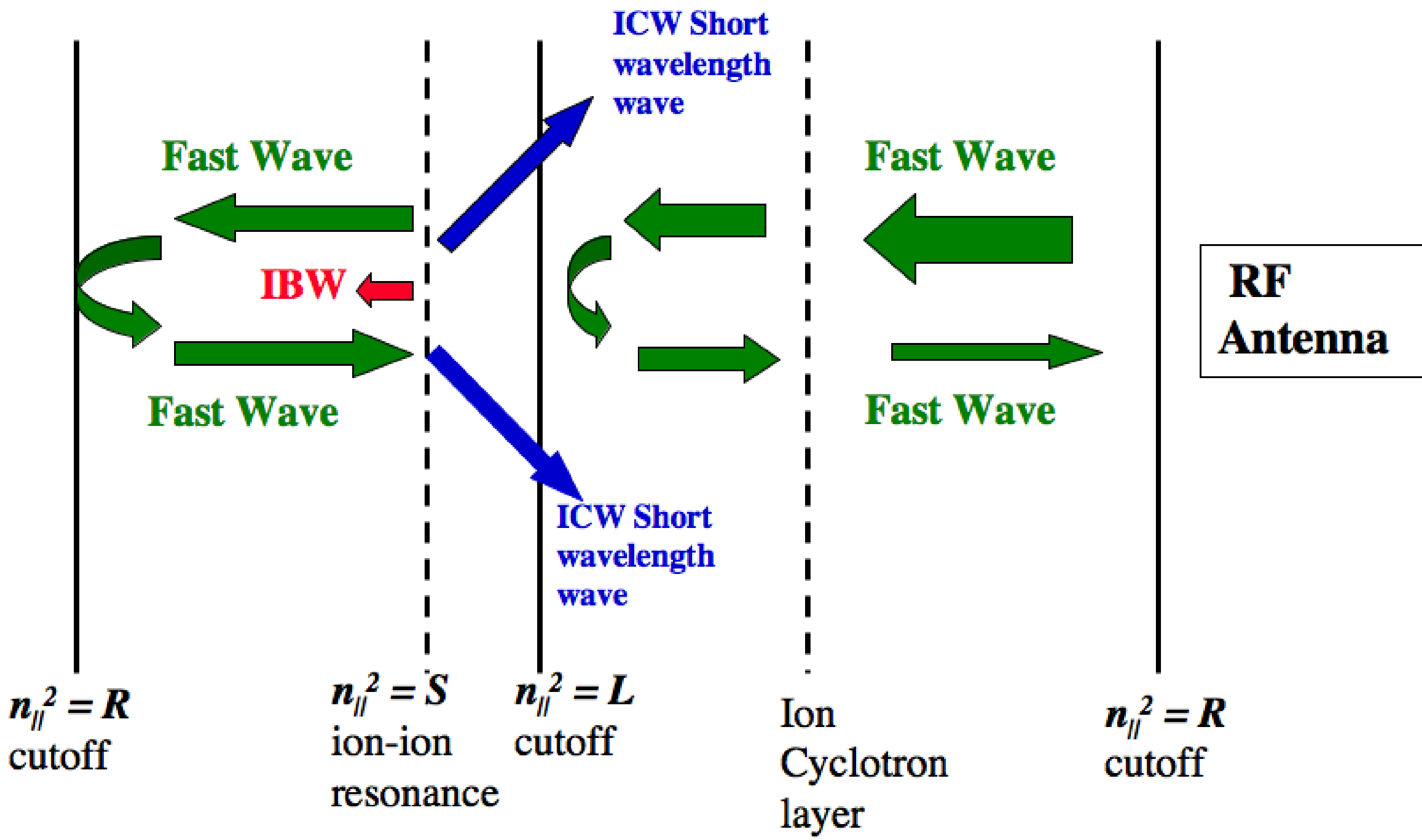

[Courtesy of Y. Lin]

Mode conversion from FW to ICW and IBW

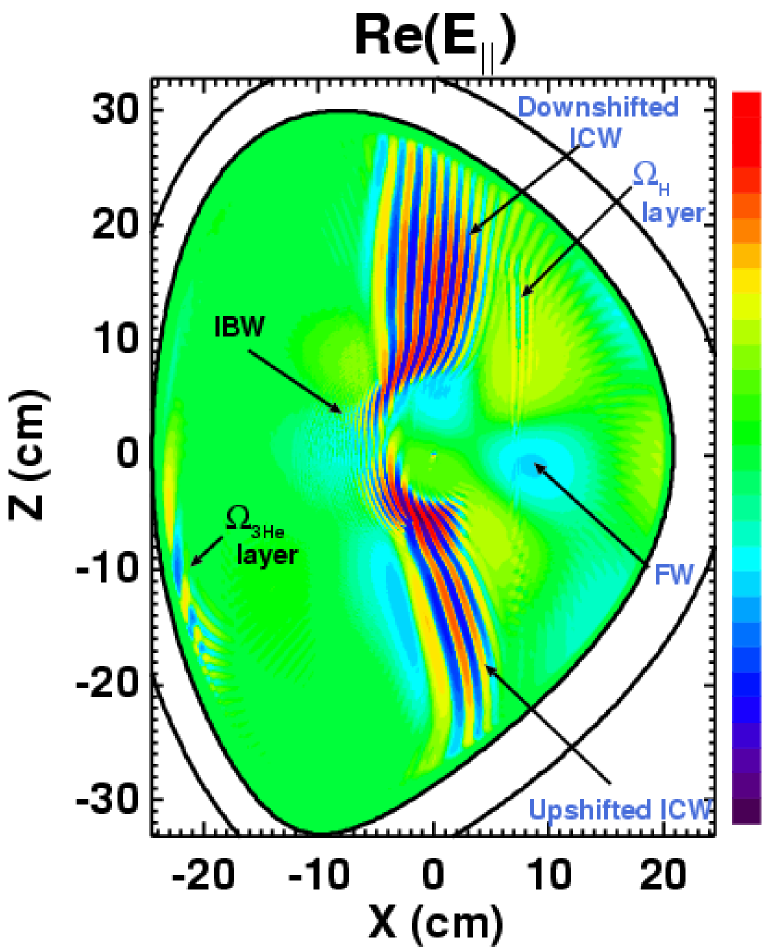

- Simulations of mode conversion are easily achieved with parallelization.(Typically Nm=255xNr=480)
- All three waves branches are apparent.
- ICW: a key example of simulation led discovery in experiments [?, ?, ?, ?]. From 'strange IBW' to 'flow drive' tool.

IBW IS ON AXIS, ICW IS OFF AXIS

- IBW electrostatics waves propagate along the midplane.
- ICW waves require a poloidal field and are coupled to off the midplane [**?**].
- FW is the large scale fluctuation. Some transmits through and reflects from the high field side cutoff.

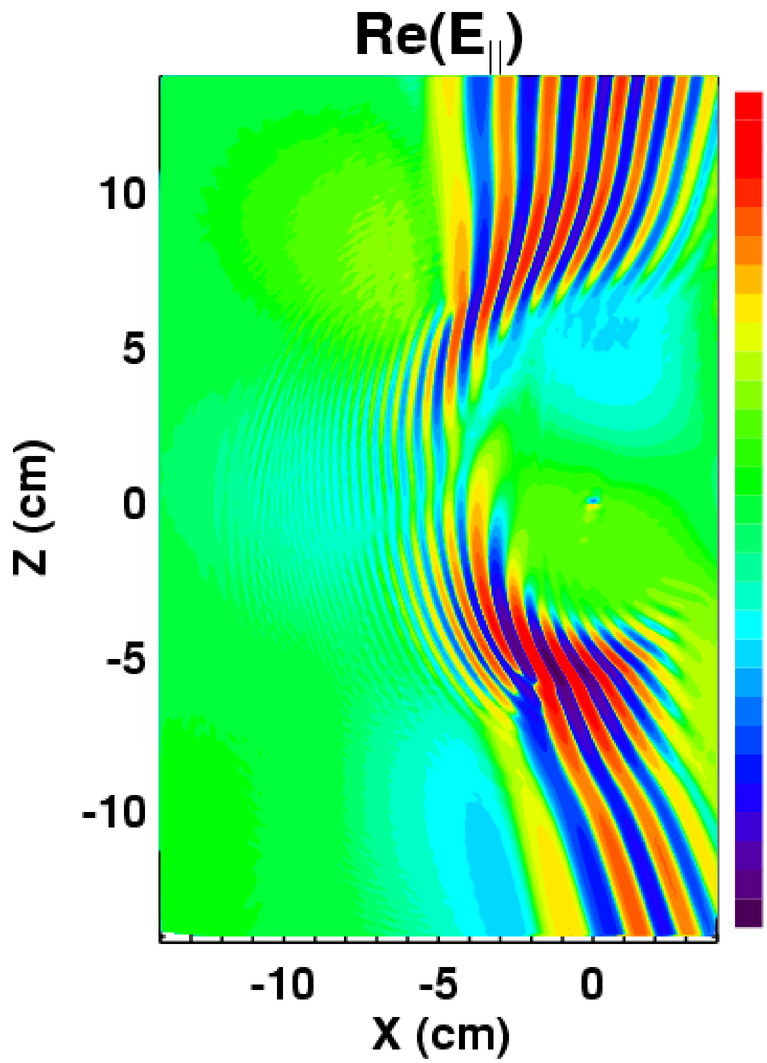

LH Absorption physics

- Parallel refractive indexes are geometrically up-shifted as waves propagate to smaller major radius. Poloidal asymmetries can cause spread in poloidal spectrum.

$$n_{\|} = \frac{c}{\omega}(m/q + n)/R$$

- Quasilinear damping occurs at $\omega/(k_{\|} v_{\rm te}) \sim 3$, and this also determines needed poloidal resolution, N_m:

$$n_{\|} \approx \frac{5.7}{\sqrt{T_e}[\rm keV]},$$

  so lower temperatures require higher $n_{\|}$ for damping.
- Higher parallel refractive indexes are more accessible to the interior of the plasma but also damp at lower temperatures=larger minor radii.
- Current drive scales as $1/n_{e0}n_{\|}^2$ and $n_{\rm acc}[n_{e0}, B]$ sets minimum $n_{\|}$ => operation in weak damping regime for $T_{e0} < 16$keV

Lower Hybrid

LHRF waves have simple dispersion relation

For LHRF Physics Regime we use cold (unmagnetized) ions and magnetized electrons.

- No FLR ion effects in unmagnetized limit: $(k_\perp \rho_\mathrm{i})^2 \to \infty$
- No electron FLR effects because of strong magnetization: $(k_\perp \rho_\mathrm{e})^2 \ll 1$

Frequency range is intermediate of ion and electron cyclotron frequencies:
$\Omega_\mathrm{ci} \ll \omega \sim \omega_\mathrm{LH} \ll \Omega_\mathrm{ce}$ where $\omega_\mathrm{LH} = \omega_\mathrm{pi}/\sqrt{(}1 + (\omega_\mathrm{pe}/\Omega_\mathrm{ce})^2)$,

The conductivity in the lower hybrid limit is given by:

$$\overleftrightarrow{\sigma} \cdot \mathbf{E} =$$

$$S\,\mathbf{E}_\perp + D\,(\mathbf{b}\times\mathbf{E}_\perp) + P\,E_\zeta \mathbf{b}$$

$$S \approx 1 + \frac{\omega_\mathrm{pe}^2}{\Omega_\mathrm{ce}^2} - \frac{\omega_\mathrm{pi}^2}{\omega^2} \approx 1$$

$$D \approx -\frac{\omega_\mathrm{pe}^2}{\omega^2}\frac{\omega}{\Omega_\mathrm{ce}} + \frac{\omega_\mathrm{pi}^2}{\omega^2}\frac{\Omega_\mathrm{ci}}{\omega} \approx -\frac{\omega_\mathrm{pe}^2}{\omega\Omega_\mathrm{ce}}$$

$$P = 1 - \frac{\omega_\mathrm{pe}^2}{\omega^2} - \frac{\omega_\mathrm{pi}^2}{\omega^2} \approx \frac{\omega_\mathrm{pe}^2}{\omega^2}$$

Estimate wavelength from slab dispersion.

Consider the lower hybrid dispersion relation corresponding to the conductivity:

$$P_4 n_\perp^4 + P_2 n_\perp^2 + P_0 = 0$$
$$P_4 = S$$
$$P_2 = (S + P)(n_\parallel^2 - S) + D^2$$
$$P_0 = P\left[(n_\parallel^2 - S)^2 - D^2\right]$$

Take the electrostatic limit $\rightarrow$
$k_\perp^2 \approx -\frac{P}{S} k_\parallel^2 \;\Rightarrow k_\perp \approx \frac{\omega_{\mathrm{pe}}}{\omega} k_\parallel$
Let's plug in some numbers:

Alcator C-Mod typical parameters

$$B_0 = 4.5\mathrm{T}, \mathrm{D}^+$$
$$f_0 = 4.6\mathrm{GHz}$$
$$n_\parallel = 2.5,\; n_a \equiv \frac{\omega_{\mathrm{pe}}}{\Omega_{\mathrm{ce}}} + \sqrt{S} = 2$$
$$n_{e0} = 2 \times 10^{20} m^{-3}$$
$$\omega/\Omega_{\mathrm{D}} \approx 125$$
$$k_\perp \approx 66\mathrm{cm}^{-1}$$

where the parallel wavenumber, $n_\parallel$ must be greater than the accessibility criterion, n_a, for the wave to penetrate into the plasma.

Lower Hybrid wave slow wave used experimentally

- Two propagating modes: fast and **slow** wave
- Wavelengths are very short
  $\lambda_\perp \approx \frac{\omega}{\omega_{\rm pe}} \lambda_\parallel \approx 1$mm
- Predicts an accessibility criterion [**?**]:
  $n_\parallel >= n_{\parallel \rm a} \equiv \frac{\omega_{\rm pe}}{\Omega_{\rm ce}} + \sqrt{S}$

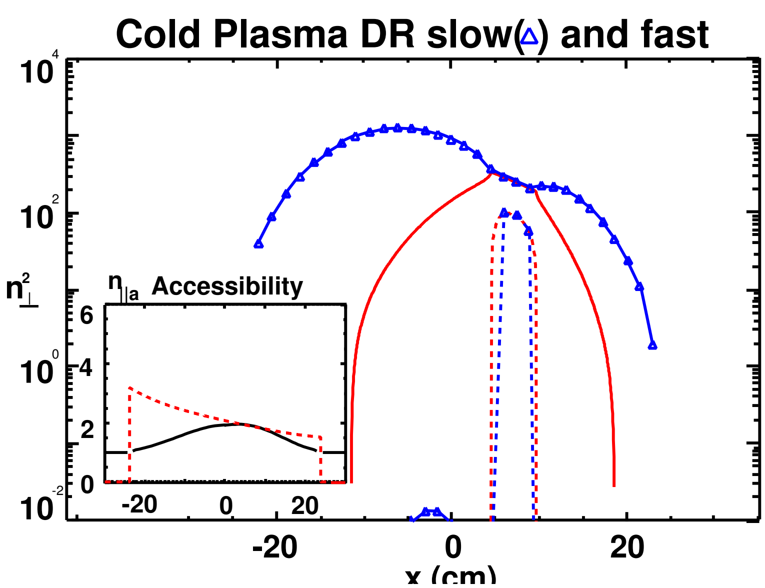

Lower Hybrid field path and ray trajectories agree

Finite electron temperature affects ray trajectory

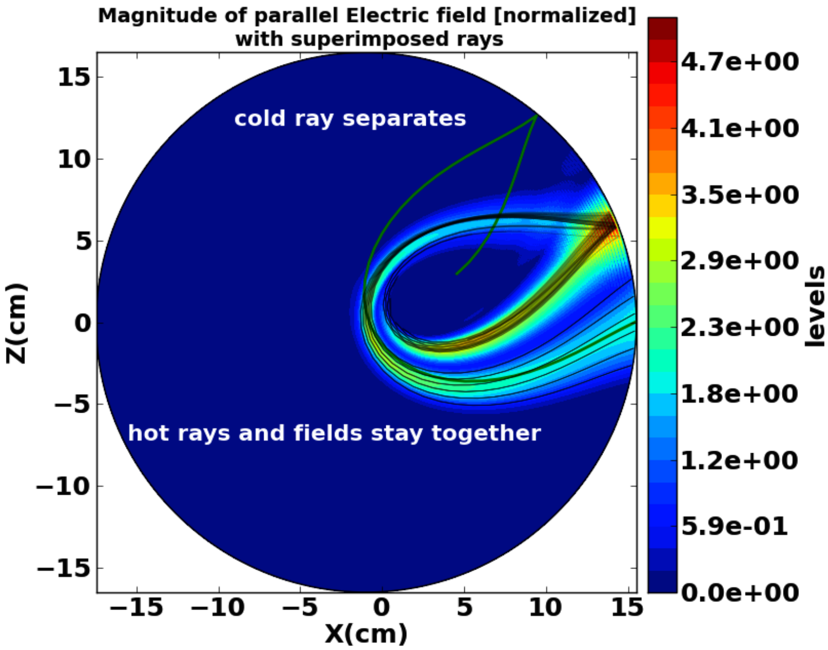

- Provided the same dielectric is used!

$$Sk_\perp^2 + P_{\mathrm{cold}} * Z\left(\frac{\omega}{k_\parallel v_{\mathrm{te}}}\right)k_\parallel^2 = 0$$

- Thermal correction is important for propagation as well as damping

Participants in the Center for Simulation of Wave-Plasma Interactions

L.A. Berry, D.B. Batchelor, D. L. Green,
E. D`Azevedo, E. F. Jaeger

ORNL — Oak Ridge National Laboratory

D. Smithe T. Austin
J. Carlsson

Tech-X

P.T. Bonoli, J.C. Wright,
H. Kohno, A. Bader, A. E. Schmidt,
G. Wallace

MIT PSFC

C.K. Phillips, E. Valeo
N. Gorelenkov, H. Qin

PPPL — Princeton Plasma Physics Laboratory

R.W. Harvey, A.P. Smirnov
Y. Petrov

CompX

M. Brambilla
R. Bilato

IPP

M. Choi

General Atomics

Politecnico di Torino
R. Maggiora

D. D'Ippolito, J. Myra - Lodestar Research

Lower Hybrid wave introduction

- Frequency range: $\omega/2 > \omega_{\rm LH} \sim \sqrt{\Omega_{\rm ce}\Omega_{\rm ci}}$
- Unmagnetized ions
- Strongly magnetized electrons
- Two propagating modes: fast and **slow** wave

- Wavelengths are very short $\lambda_\perp \approx \frac{\omega}{\omega_{\rm pe}}\lambda_\parallel \approx 1{\rm mm}$
- Predicts an accessibility criterion: $n_\parallel >= n_{\parallel{\rm a}} \equiv \frac{\omega_{\rm pe}}{\Omega_{\rm ce}} + \sqrt{S}$

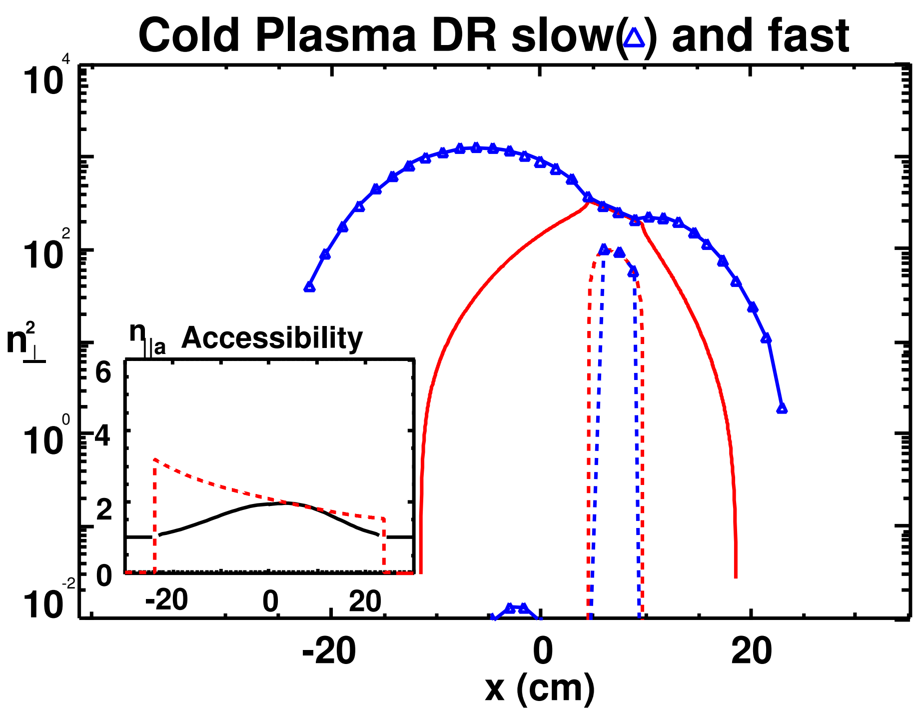

Phase Contrast Imaging diagnostic measures ICRF waves 'directly'

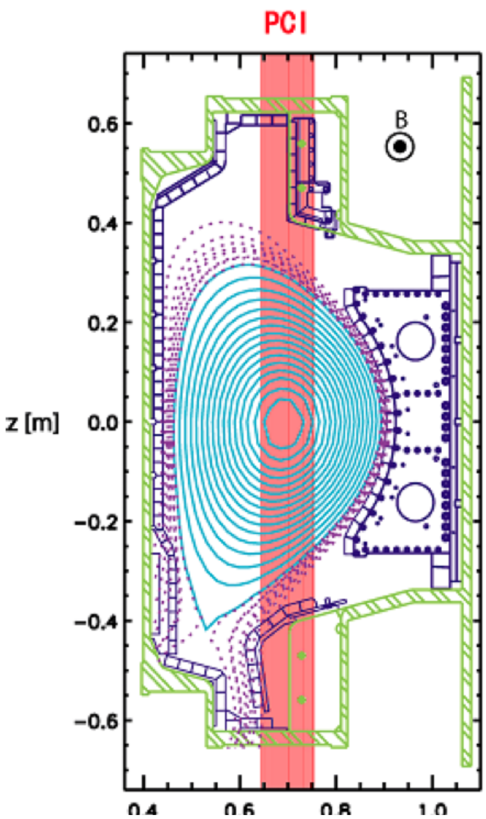

- PCI measures phase fluctuations in RF electric field and relates those to density fluctuations by scattering.

$$I_{\mathrm{PCI}} \propto \|E_0\|^2(1 + 2\tilde{\phi}) \sim \int dz\, \tilde{n}_e$$

- Density fluctuations in synthetic PCI are related to electric field through the electron momentum equation. More sophisticated model using consistent kinetic conductivity have been also implemented: [cite Nstujii]

$$n_e = \frac{i}{e\omega} \nabla \cdot (\sigma_e \cdot E)$$

Synthetic PCI comparison with experiment

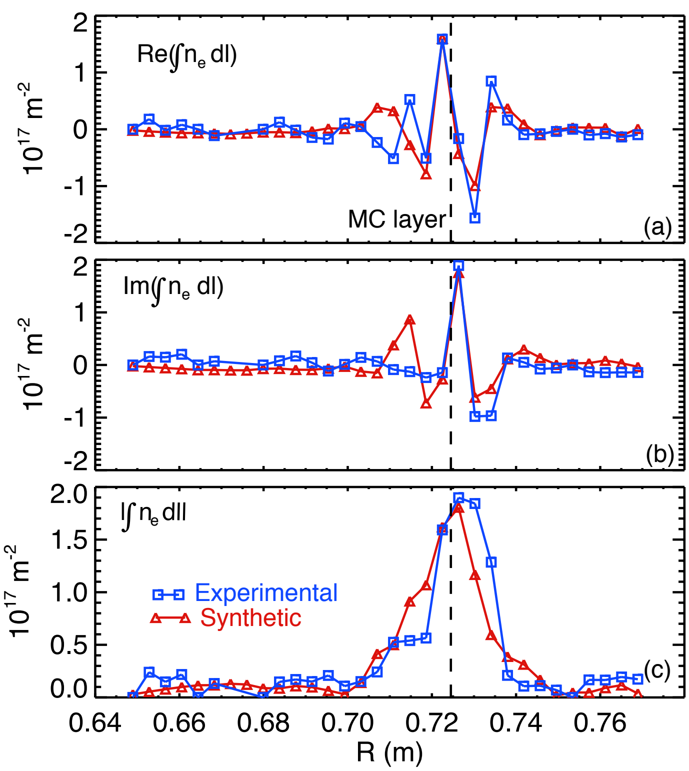

- Phase contrast imaging diagnostic is used to look at density fluctuations from ICRF waves on C-Mod
- Cases a) and b) show the real and imaginary part, c) the magnitude.
- Synthetic diagnostic identified aliasing in earlier verison of PCI with fewer channels [Lin 2004]
- Good agreement in some cases but not others. Possible edge effects, 3D uncertainty from antenna phase, uncertainty in minority concentration.

Ion Cyclotron Absorption with Nonthermal Ion Tail Production

If “minority” ions species (eg 5% H) is present in a “majority” ion species plasma (95% D) then an RF wave with $\omega = \Omega_H$ will have an electric field component with the same polarization as the minority ion:

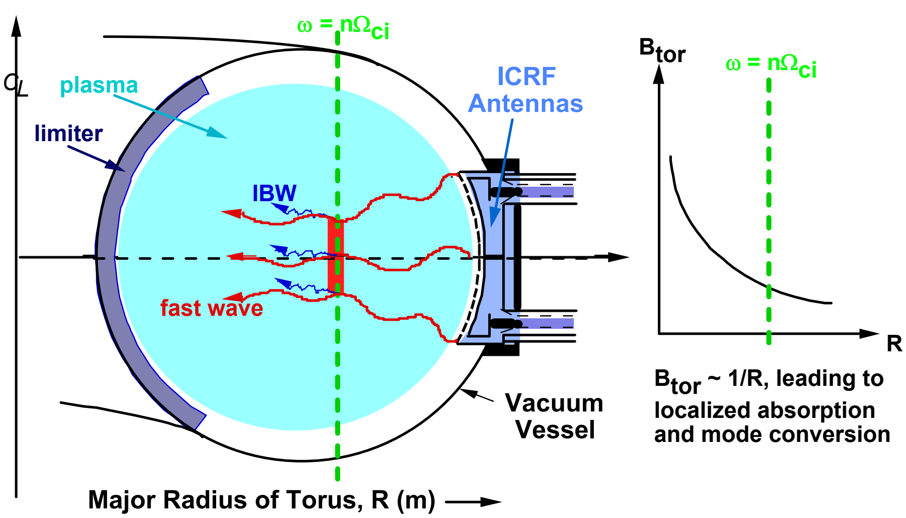

- Secular interaction - wave damps its power via cyclotron absorption on the minority ion.
- Nonthermal, anisotropic minority ion tail is generated that slows down and heats background electrons (drag) and majority ions (collisions).

MINORITY HEATING EXAMPLE SHOWS INTENSE FIELDS AT RESONANCE [AORSA SIM].

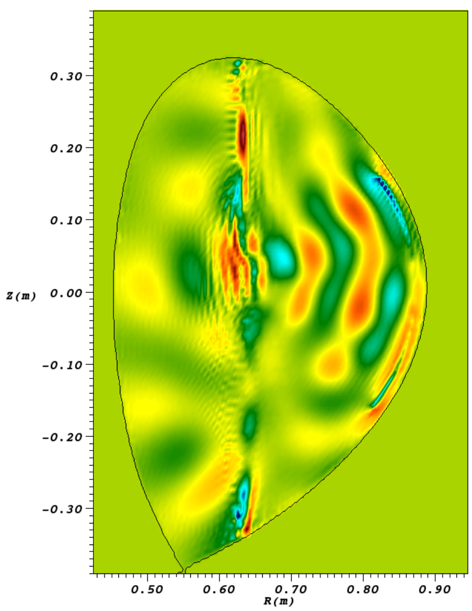

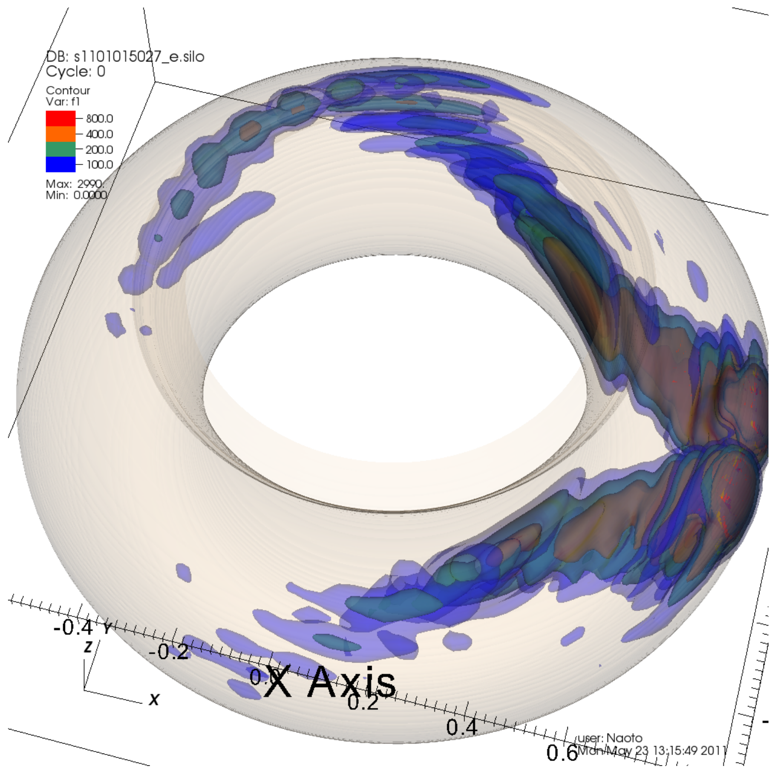

- Wavelengths on the order of several cm.
- Multipass nature of minority heating apparent in the 3-D rendering.
- 3-D fields obtained by superposing results from 40 toroidal modes.

Proof of concept 2D - mode matching

Propagation in 2D stratified media

- Direct solution in COMSOL:

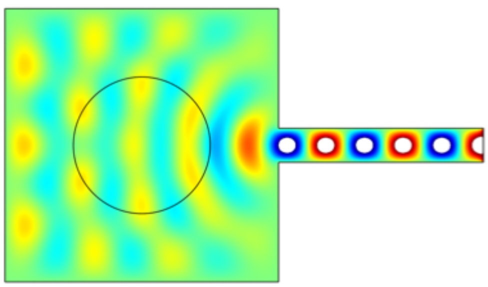

- Mode-matching solution (modal excitation done in COMSOL, superimposition done in MATLAB)

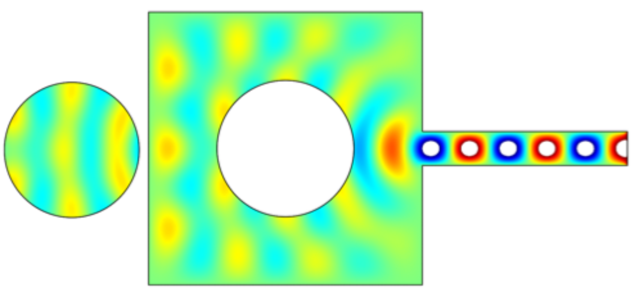

Comparison of modal content between direct solution and mode-matching solution

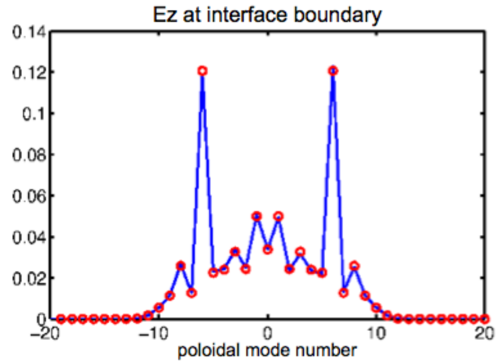

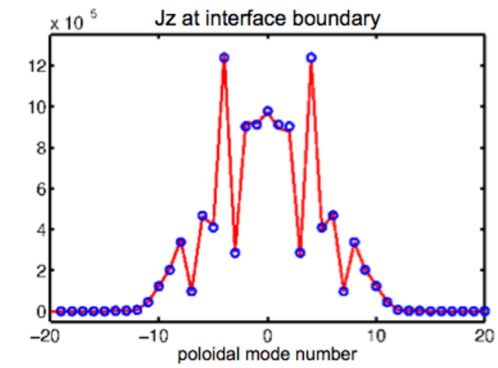

[Shiraiwa and Meneghini 2010]

Simple example of Mode Matching

Propagation in a 2D stratified isotropic lossy medium

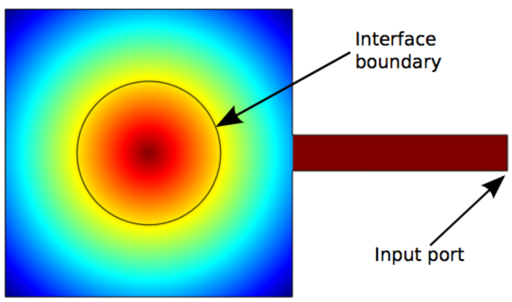

- Direct solution: solve the problem at once in FEM code, COMSOL
- Mode matching solution:
  - Split the problem into two regions:
  - Core region (cylindrical)
  - Edge region (complicated shape, includes walls and wave launching structure)

  - Modal excitation
  - 2D $\rightarrow$ $\mathbf{E} = E_0 \hat{z}$
    single longitudinal mode $n = 0$
  - 41 polarmodes $20 < m < 20$
- At the cylindrical interface polar modes are well defined
- Cylindrical geometry does not couple the modes to one another

[Shiraiwa and Meneghini 2010]]

Proof of concept 2D - mode excitation

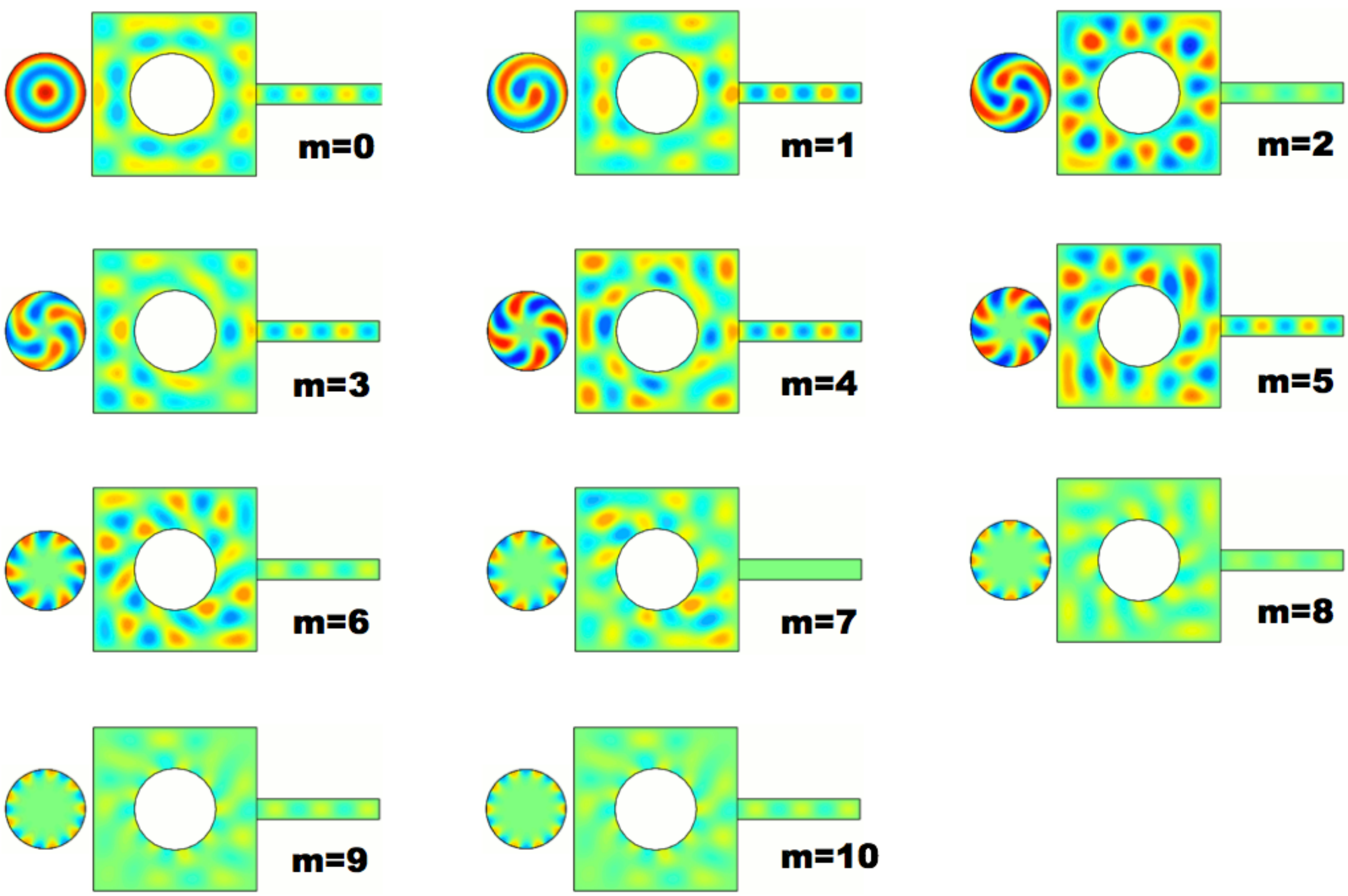

TORIC geometry in COMSOL

- TORIC uses flux coordinate system
  - θ (poloidal), ψ (radial), and ϕ(toroidal)
  - Basis vectors for E, B fields are normalized.
  - Mode is exp(imθ + inϕ)
- COMSOL
  - R, Z, phi coordinate system
  - Mapping from θ to geometrical θ_g

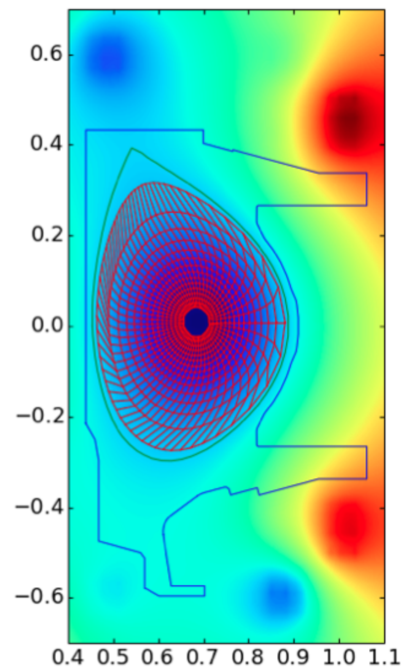

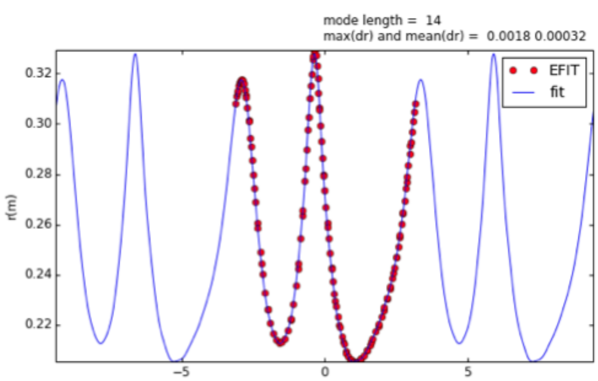

Last closed flux surface is represented by
R0 + $a(\theta_g)\cos(\theta_g)$, Z0+$a(\theta_g)*\sin(\theta_g)$

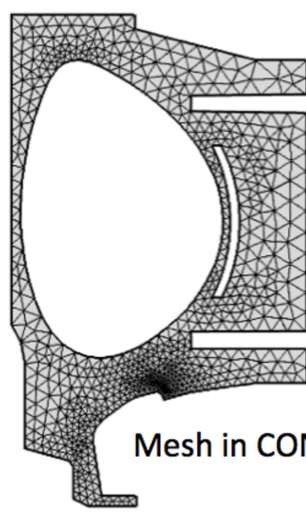

Mesh in COMSOL

C-Mod $n_{\|} = -3.1$

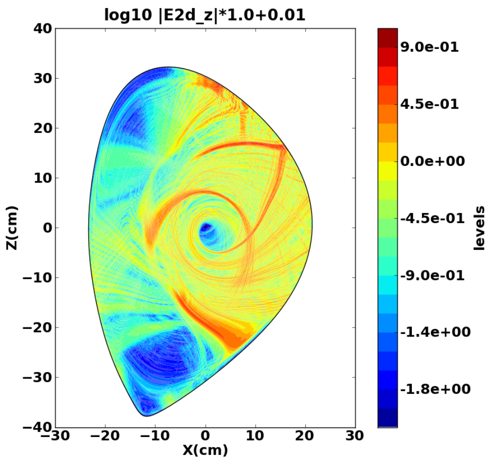

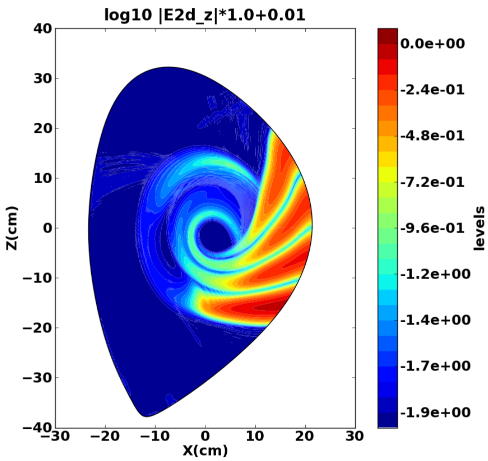

/home/jwright/TORIC_RUNS/618/Step13/TORICLH.cdf

- Upper left initial
- Lower left converged
- Upper right converged spectrum
- Lower right converged power

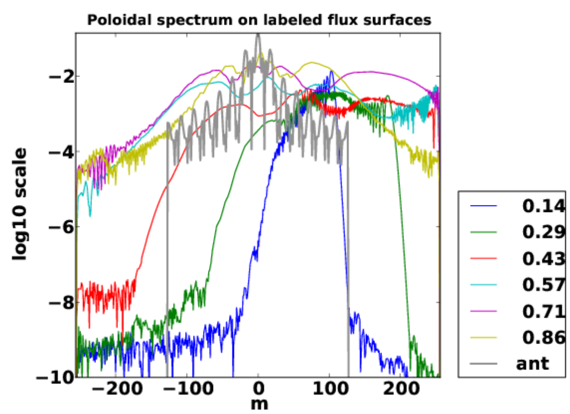

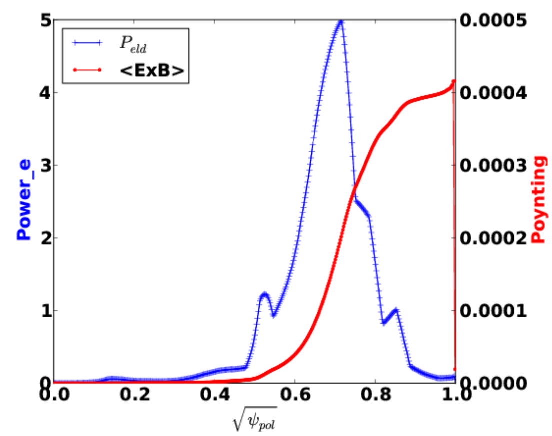

HXR diagnostic on Alcator C-Mod

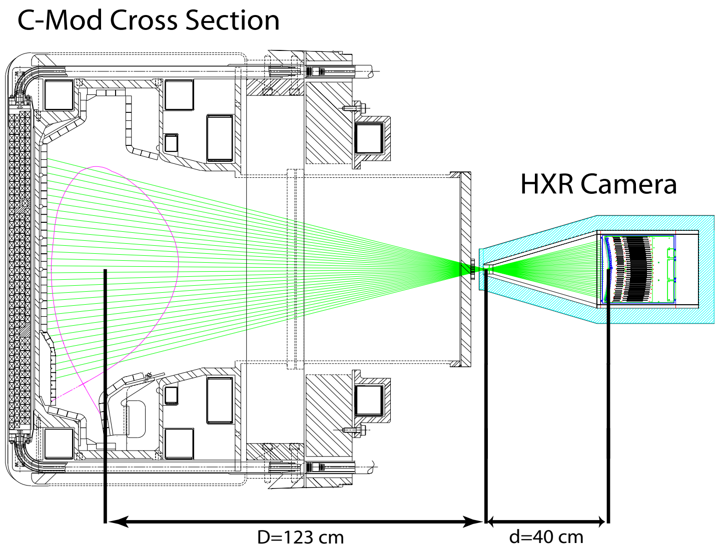

Figure Courtesy John Liptac

- 32 chords, measures X-rays from LH accelerated electrons that have been pitch angle scattered
- A synthetic hard X-ray diagnostic in CQL3D uses the same geometry to produce a signal for comparison.

HXR comparison using synthetic HXR

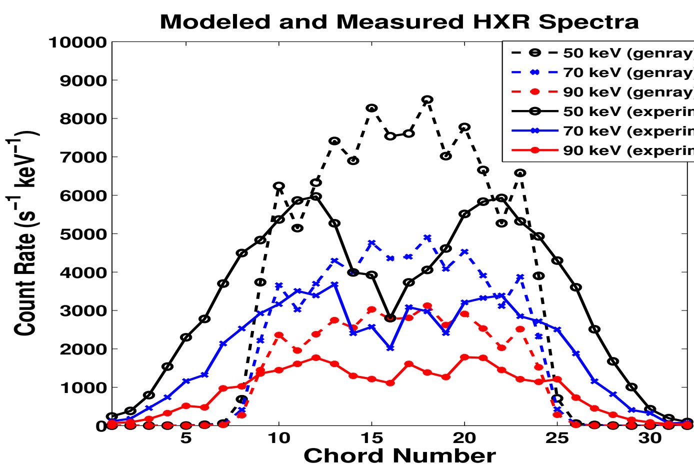

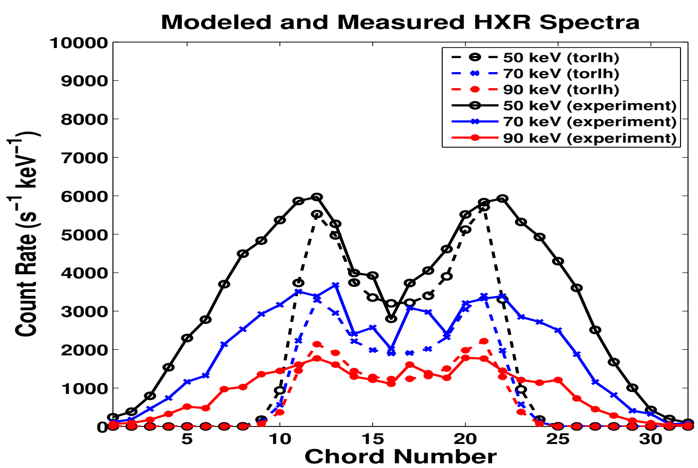

[Schmidt Diss. 2011]

- Comparison of measured and modeled Hard X-Ray emission profiles for Alcator C-Mod LH experiment 1060728011 with $n_{\|} = -1.55$.
- Modeled profiles from ray tracing (left panel) have been scaled by a factor of 1/5 and those from full wave (right panel) have not been scaled. Differences are due to interference effects present in full wave simulations.
- Note that both and are narrower in spatial extent than experiment.